Escola de Camins
Escola Tècnica Superior d'Enginyeria de Camins, Canals i Ports
UPC BARCELONATECH

PROJECTE O TESINA D'ESPECIALITAT

Títol

Seismic design of stainless steel structures

Autor/a

Albert Jané Toset

Tutor/a

Esther Real Saladrigas i Itsaso Arrayago Luquin

Departament

Enginieria de la construcció

Intensificació

Anàlisi i Projectes d'Estructures

Data

Juny 2014

Seismic structural design with stainless steel

Albert Jané Toset

Advisors:
Esther Real Saladrigas
Itsaso Arrayago Luquin

Departamento de Ingeniería de la Construcción

E.T.S. de Ingenieros de Caminos, Canales y Puertos de Barcelona

Universitat Politècnica de Catalunya

Barcelona, June 2014

Abstract

Title: Seismic design of stainless steel structures
Author: Albert Jané Toset
Advisors: Esther Real Saladrigas and Itsaso Arrayago Luquin
Key words: Earthquake, seismic design, stainless steel, framed structures, modal analysis, pushover analysis

Stainless steel has not been used as a structural material since last decades. Mainly, it was used for the alimentary and automotive industry or for hygienic applications because of its corrosion resistance property. But, another determining stainless steel property is its ductility, a very interesting aptitude to achieve a good structural response against the seismic action. This ability to deform while keeping or increasing the resistance, makes stainless steel a candidate to be used for seismic design.

There are different seismic standards to take into account the effect of earthquakes in the structural design, such as EN-1998 or NCSE-02, but these standards do not consider the possibility of using stainless steel and its advantages. That is why, in this study has been compared the overstrength values given by the standards with the values obtained with the computed models.

12 pushover and modal analyses have been carried out in order to be able to grasp carbon steel and stainless steel behavior against the seismic action. Two frame typologies have been studied: regular moment resisting frames and concentrically braced frames. The study includes a comparison between carbon and stainless steel behavior against the seismic action, a checkout to see if the overstrength values given by the EN-1998 are valid for stainless steel and if it worth the additional cost of stainless steel regarding to the overstrength achieved.

These analyses show the suitability of using stainless steel in the seismic design. Stainless steel frames show higher values of ductility and overstrength than carbon steel. The economic study shows that the direct cost of stainless steel is higher than carbon steel but with an accurate design is possible to achieve a higher increment of overstrenght than the additional cost of using stainless steel.

In the majority of the cases the overstrength values given by the standards are reasonable and secure. But, in some cases, the overstrength values given by the standards can be too optimistic thus leading to an insecure design of the frame. So, structural designers must be careful and choose a cautions overstrength value.

Hence, the obtained results show the structural benefits of using stainless steel and highlight that stainless steel has a long way to go in seismic design.

Acknowledgements

I would like to thank my advisors, Esther and Itsaso, for the opportunity of discovering two completely new fields for me, the stainless steel and the seismic action. I would specially thank Itsaso for all her support during the curse and her help in this study.

I would also like to thank to my mates I met during these six years in the school: Leire, Cristina, Lleó, Eric, Blanca, Gerard, Francesc...

Finally, I would like to thank to my family and Irene. Without their support all this would not has been possible at all.

Table of contents

List of figures

List of tables

1. INTRODUCTION

1.1. Background and motivation

Earthquakes have been caused a devastating effect along the history of the humanity. Many civilizations have suffered to overcome the seismic destruction. In the past, it was believed that the earthquakes were a divine punishment because the gods were angry. Fortunately, nowadays, there is enough knowledge about earthquakes to predict the seismic event that could be presented and the economic loses that this hypothetical seism could cause.

Humans have been trying to build more resistant buildings, especially after a severe seismic event. But it could be demonstrated that after three generations the seismic memory of the population of seismic zone vanishes, and the same mistakes made in the past reappears. That is why, actually, some countries have developed seismic standards. Logically, the countries with an elevated seismic action has written the most precise standards and they made them earlier than countries with a low seismic action.

Most of the buildings and constructions around the world are made of concrete. The second most used structural material is carbon steel. That is why seismic standards only consider these two materials.

Because of stainless steel properties it is predictable that its use can suppose a sustainable benefit regarding seismic performance. Hence, needless to say that in this field stainless steel has a long way to go.

Stainless steel is a relatively recent material which has been used for several applications and nowadays is raising its application by the construction industry. The excellent combination of mechanical properties and the corrosion resistance makes stainless steel a very good material for structural applications. The complexity of its behavior has made stainless steels presence in construction industry particularly low.

Due to the lack of existing design rules for stainless steel the rules for carbon steel have been generally applied in the stainless steel design. But the marked non-linear behavior of stainless steel, which is the main difference with carbon steel, makes the standards for carbon steel not always acceptable in the stainless steel design. In fact, stainless steel presents a better behavior against the seismic action due to its ductility.

Over lasts decades much research has been done in this field in order to achieve a better understanding of the stainless steel behavior, as well as to check the applicability of the existing specifications, and to obtain new designing rules to provide the designers with more efficient ways of designing.

1.2. Scope of this study

The principal aim of this work is to evaluate the benefits of using stainless steel in framed structures against the seismic action. The study might comprehend a rigorous study of different frames to be able to give some conclusions about the suitability of stainless steel in seismic design. For this purpose, it is expected to run non-linear analysis and to be able of modelling the non-linear stainless steel behavior properly.

1.3. Outline and content

In Chapter 2, there are summarized the main concepts of the seismic action that has been considered essential for the proper understanding of the present work. A general overview of the existing literature about stainless steel studying the material properties and qualities is given as well.

Chapter 3 contains a description of the analysis that has been run (modal analysis and pushover analysis) and the results of the calibration that has been carried out to be able of giving confident results. The models used and the calculus hypothesis are presented and explained too.

In Chapter 4 the results of the cases of study are presented, analyzed and commented. The main results of this study have been the fundamental period of the studied frames and whose capacity curves.

The conclusions and outlooks of this work are provided in Chapter 5.

2. STATE OF ART

2.1. Seism

2.1.1. Introduction

Humanity has experimented along the history the devastating effect of earthquakes. In the twentieth century, these natural disasters have caused an annual average of around 14000 deaths, more than caused by other natural disasters such as cyclones, hurricanes, floods, avalanches and volcanic eruptions. Furthermore, geophysical events cause significant economic losses like public infrastructure and private buildings damage, which has a negative impact on the development of affected areas. In Figure 2.1 can be seen the distribution of human deaths caused by natural disasters and the economic losses produced by each one.

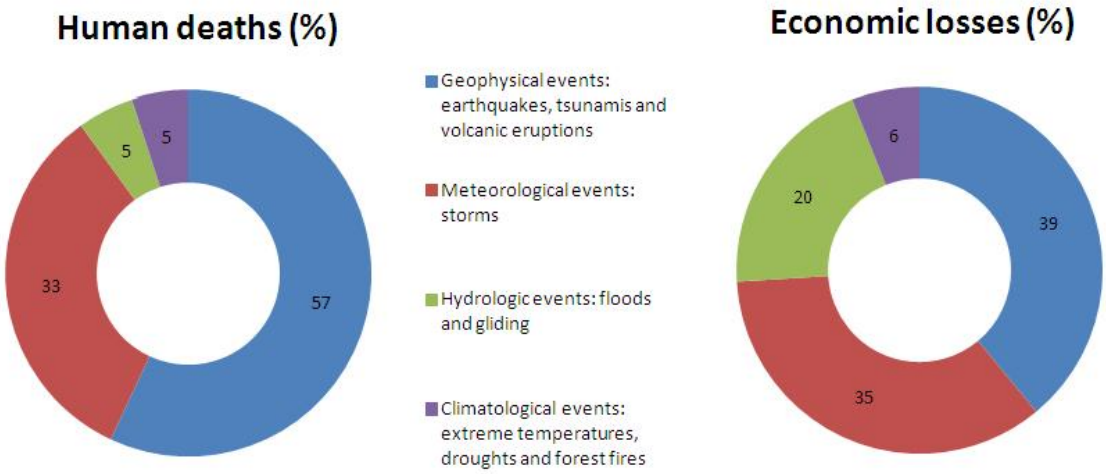

Figure 2.0.1. Human deaths and economic losses caused by natural disasters. Munich RE (2012)

This data has been obtained from the 300 major natural disasters in the world between 1950 and 2011 and provided by Munich RE, an insurance company. The total deaths reached the value of 2.400.000 and the total economic losses had been of 2,4 billions of American dollars. From this data is concluded that geophysical events are the main cause of economic losses and human deaths in the world.

2.1.2. Magnitude and intensity

All of us, at least once, have heard or read about earthquakes in the news or in newspapers. Commonly, they use words like magnitude or intensity. In this section these words are defined and explained. These two concepts were born in order to define the severity of earthquakes.

The magnitude of an earthquake is a quantitative measure of the energy released in the form of seismic waves. This concept was first introduced by Richter (1935). He wanted to compare the released energy in the focus of different earthquakes. The total released energy of a seism is the sum of the energy transmitted by seismic waves and

the energy released by other phenomena, mainly heat. The released energy of seismic waves is between 1% and 10% of the total energy. For this reason, Richter considered that the amplitude of seismic waves is almost a measure of the total energy of a seism and establishes for the local magnitude the following expression Eq. 2.1:

$$M_L = \log A - \log A_0 \tag{2.1}$$

Where A is the maximum amplitude registered by a torsion seismometer Wood-Anderson at a given distance, and A_0 is a function of attenuation corresponding to an earthquake taken as benchmark.

Hence, magnitude is a value that only depends on the seism itself and not on the associated damage.

The values of the magnitude have a physical limit given by the characteristics of the earth materials. This limit has not exceeded the grade 9 on the scale of Richter, for now. Later, Gutemberg and Richter also proposed similar expressions to evaluate the magnitude from superficial waves and internal waves.

On the other hand, intensity is a qualitative measure of the effect at a given location due to an earthquake. It takes into account buildings and structures damage, consequences on the area and consequences on people. There are two ways of determining the intensity, subjectively or analytically. The first one is the most extended method.

To evaluate the intensity subjectively more than 40 scales have been proposed around the world. The most used and relevant could be these ones: Rossini Forel (1873), Mercalli (1902) and modified Mercalli (MM 1931, 1956, 1965), Mercalli-Cancani-Sieberg (MCS 1917, 1942) and Medvedev-Sponheuer-Karnik (MSK 1964, 1992). The MM is the most used in the American continent and MSK is the most used in Europe.

Moreover, one example of measuring intensity analytically is the intensity of Arias, based on the potential of damage, and it is independent of the existence of buildings in the affected zone. The expression shown in Eq. 2.2 is valid for values of critical damping between 2% and 20% (Sarria 1990).

$$I_a = \frac{\pi}{2g} \int_0^{t_0} a^2(t) dt \tag{2.2}$$

Where t_0 is the earthquake duration and a is the acceleration.

2.1.4. Seism: design action

The seismic problem is a purely dynamic problem, although the first methods for his consideration were based on static concepts. So, the method of equivalent static forces arose. Most of seismic standards use this method for regular and simple buildings. The development and dissemination of computers and structural analysis programs has allowed a widespread implementation of dynamic methods for seismic action. These

methods, depending on the type of analysis to make, use accelerograms or spectrums of acceleration and capacity curves.

There are two procedures to evaluate the seismic potential of a specific zone: the deterministic and the probabilistic one.

The deterministic method considers that future seismicity will be the same as in the past. The strongest drawback about this method is that the historical maximum has not to be necessarily the maximum in the future. That is why the more seismic data is available, the more correct these historically based methods are.

Probabilistic methods are based in the fact that from historical seismicity can be established statistical laws that define seismic characteristics of a zone (Udías and Mézcua,1968).

Anyway, most of seismic standards usually take into account the seismicity of the region, the characteristics of the soil foundation, the importance and utility of the structure, and the main characteristics of the structural response, such as ductility and overstrength. Seismicity of the region and characteristics of soil foundation are defined by a design spectrum, usually of horizontal accelerations. The importance of the building and its utility is taken into account by a coefficient that increments the action for public infrastructures or high occupation buildings. The main characteristics of structural response are represented by a response coefficient (β, in NCRS-02 (2002), the Spanish seismic standard) that tries to represent ductile performance and overstrength.

Seismic standards usually set the minimum requirements to ensure the protection of human lives, which means to avoid partial or total collapse of the structure but, without controlling the building damage.

Earthquake resistant structures, except in special cases, are designed to respond in inelastic range, in order to develop ductility and dissipate energy during the occurrence of a severe earthquake. The development of ductility involves the occurrence of structural damage as a result of steel yielding. Some instability problems like local buckling can happen too eventually in steel buildings. This damage can have an important repairing cost, which can be significant depending on the type and quantity of the affected elements, repairing technics, etc.

This criteria differs from the one applied to lateral wind actions, where the structure is designed in order to remain essentially in the elastic range. The main reason for this difference is basically economical, construction cost must be reasonable. That is why the forces obtained from the design spectrum are reduced by a response modification factor, R or q depending on the standard, which mainly considers the effect of ductility and overstrength system. Capacity curves need to be explained to understand properly the origin of this coefficient.

Hence, response spectrums and capacity curves are explained in the following sections.

2.1.4.1. Accelerograms

Seismometers are instruments that measure the ground movement. They can register what are called accelerograms. In Figure 2.2 the accelerogram of Lorca's earthquake (Murcia, Spain) is shown.

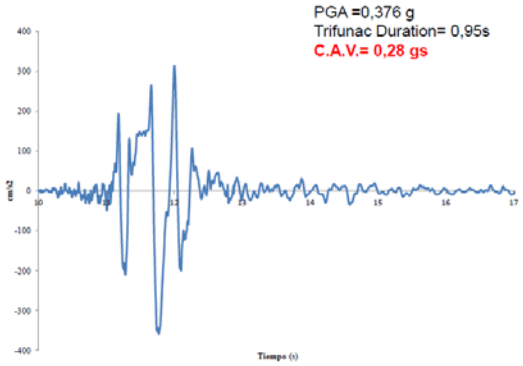

Figure 2.0.2. Lorca's accelerogram. IGC (2011)

Accelerograms show the evolution of the ground acceleration against time. There are some significant values that can be obtained from accelerograms and usually are used to define an earthquake. The most characteristic value obtained from an accelerogram is the peak ground acceleration. PGA is the maximum acceleration registered in an earthquake and is usually given adimensionalized by the gravity acceleration.

It can be observed that there is not a clear beginning and clear end of the earthquake. So, it is difficult to define its duration. In certain works, such as Bolt's (1985), it is proposed what he called the bounded duration, which is defined as the time span that the shaking of the earthquake remains above a certain threshold acceleration, usually 0,05g.

Other authors take into account the shape of the accelerogram and not acceleration levels. They find correlations between the effective duration and the magnitude of an earthquake. Trifunac and Brady (1975) got this duration with maximum energy of motion and defined the concept of effective duration as the time of the intensity function of Arias (2) for exceeding 5% and reaching 95% of its value. In Figure 2 this datum is shown for Lorca earthquake. Dobry and Idriss (1978), after studying more than 84 accelerograms registered in the west of USA, found that for magnitudes between 4,7 and 7,6, and focal distance between 0,1 Kilometers and 130 Kilometers, the following regression shown in Eq. 2.3 is valid.

$$\log t_d = 0{,}43M_L - 1{,}83 \qquad (2.3)$$

Where t_d is time, measured in seconds, and M_L is the seism magnitude.

Another value that can be obtained from accelerograms is the cumulative absolute velocity and is defined as the integral of the absolute value of an acceleration time series as it can be seen in Eq. 2.4.

$$CAV = \int_0^{t_{max}} |a(t)| dt \quad (2.4)$$

Where t_{max} is the total duration of the time series.
From this equation can be deducted that CAV includes cumulative effects of ground motion duration. Therefore, it is a value that correlates fairly well ground motion with structural damage. In Figure 2.2 this value is also shown.

As a rule, accelerograms are used for advanced calculating methods, like dynamic analysis.

2.1.4.2. Response spectrum

Generally, a spectrum could be defined as a graphic with the maximum response that an action can produce to a structure or an oscillator of one degree of freedom. This maximum response can be velocity, acceleration, displacement or whatever is studied.

Elastic response spectrum represents the maximum of a parameter of study (in this case, acceleration) for simple oscillators of one degree of freedom with a vibration period (T) and a dumping coefficient.

In Figure 2.3 a response spectrum can be seen. It has three curves, with a different dumping coefficient each. In this figure, the dumping coefficient is represented by the letter "ξ", but in the Spanish standard it is used letter "υ". The less the dumping coefficient, the more spectral acceleration.

This kind of spectrum cannot be used for design because it is made by only one acceleration record. That is why seismic standards use design spectrums that consider the seismic hazard of the zone and they are defined by smoothed curves. These spectrums can be obtained by a probabilistic or deterministic procedure. In Figure 2.4, as example, the design spectrum of NCSE-02 (Spanish standard) is shown.

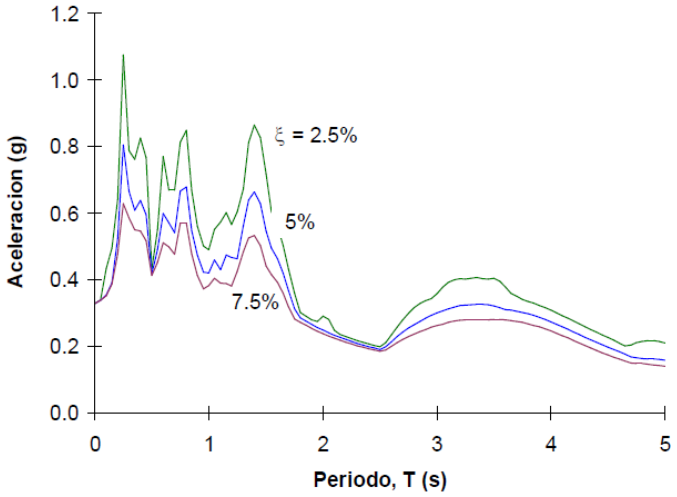

Figure 2.0.3. Elastic response spectrum, earthquake in Turkey. Crisafulli (2012)

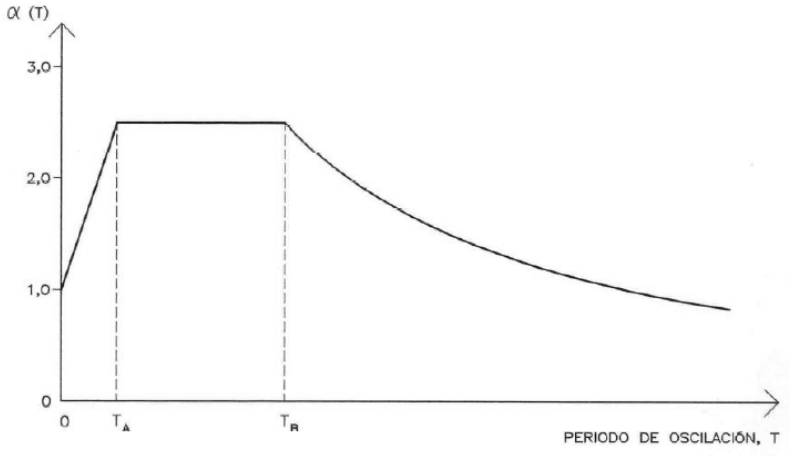

Figure 2.0.4. Design spectrum of NCSE-02 (2002)

2.1.4.2. Capacity curves

Capacity curves define the seismic performance of a building. This graphics usually shows the roof displacement against shear stress in the base. In Figure 2.5 there is an explicative example.

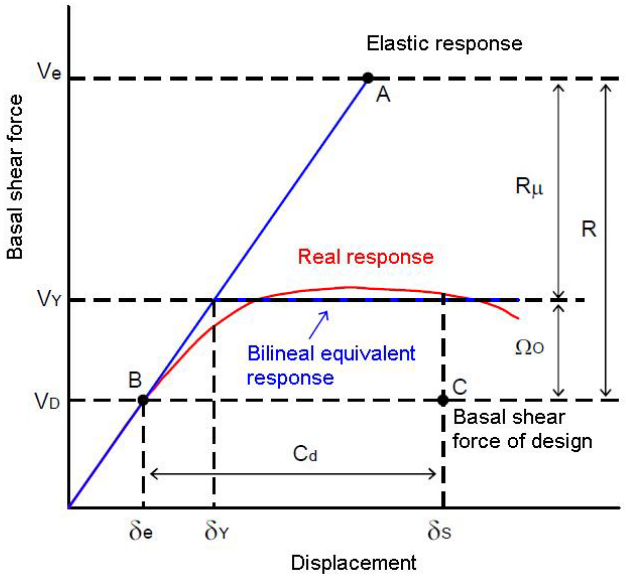

Figure 2.0.5. Capacity curve. Crisafulli (2012)

As it can be observed the design shear force in the base is lower than the real resistance of the building before reaching failure. The strength level defined by the design spectrum is represented by the basal shear force, V_e, the design basal shear force is V_D. At this point, the structure leaves the elastic and linear behavior. The R coefficient reduces forces from serviceability limit state to the ultimate state. The overstrength factor, Ω_0, takes into account the reserve of strength between V_D and V_Y. V_Y could be defined as the ultimate basal shear force of the structure. This overstrength arises from structural redundancy, overstrength of materials, oversizing of

structural members, different load combinations for seism, limit of interstorey distortion, etc. In Figure 2.6 there is a scheme of lateral displacement and interstorey distortion for seismic action.

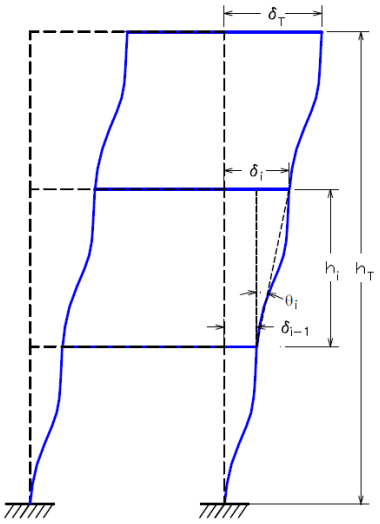

Figure 2.0.6. Lateral displacement and interestorey distortion. Crisafulli (2012)

The coefficient R, overstrength Ω_0, lateral displacement and interstorey distortion are used in seismic standards.

2.1.3. Seismic hazard

For studying earthquakes, concepts like seismic hazard, vulnerability and seismic risk are indispensable to evaluate them objectively.

It is important to differentiate the three following aspects to study objectively an earthquake. The first one is the earthquake itself: where, when and how the seism happens. The second one is the ground movement associated to the seism, and the third one is the effect of the seism to the buildings and infrastructures. The first two show the seismic hazard of a specific place and the last one talks about vulnerability, which can be defined as the susceptibility of a building of suffering damage by the occurrence of a destabilizing phenomenon, whether it is from a natural or human origin. Another important concept about earthquakes is the seismic risk, which can be understood as a magnitude of the potential losses (economic, social, environmental…) that can be caused by earthquakes in a specific region. More technically, seismic risk arises from an interaction between seismic hazard and vulnerability.

Hence, it is very important not to confuse seismic hazard with seismic risk. The seismic hazard is the potential of the earthquake that can take place in terms of shaking and the seismic risk is the potential consequences that seismic activity can cause. So, there can be a scenario with a high seismic hazard but with a low seismic risk, for instance, a rich country with buildings constructed under good seismic resistant standards. But, in the other hand, unfortunately there are countries with a low seismic hazard but with a high seismic risk; for example poor countries with precarious buildings. And from this last consideration the concept of the resilience is deduced. Resilience could be defined

as the ability of a region or a country to recover from an earthquake or another natural disaster.

Year by year damage caused by geophysical events is rising because humans are constructing in zones with high seismic hazard. Nowadays it is impossible to modify the seismic hazard, but engineers can improve the buildings response when an earthquake takes place. This fact means that engineers can act by reducing the vulnerability.

There have been some myths about seismic engineering that definitely are not true. The first one is: nothing can be done when a very strong earthquake takes place. And the second one: extreme events will cause disasters. If the structures have been designed taking into account the seismic action these two myths collapse under its own weigh.

2.1.5. Seismic design with steel

Structural steel is a stiff, resistant and ductile material. Ductility is the ability of deformation keeping resistance. It is produced industrially which assures a properly quality control. These characteristics make it an adequate material for seismic design. In Figure 2.7 some stress-strain curves are shown for different steel grades for construction steel.

The linear part of the curve is the elastic region and its slope is Young's Modulus (for structural steel is 210000 N/mm^2). After reaching the yield point, the curve usually keeps horizontal or decreases slightly because of the relocation and redistribution of the steel molecules. As deformation continues, the stress increases on account of strain hardening until it reaches the ultimate strength, F_u. Therefore, steel is usually defined by the yield stress and strain (F_y, ε_y) and ultimate stress and strain (F_u, ε_u). As the yield stress increases, the ductility and overstrength usually decreases. The ductility of a material can be defined as it is shown in Eq. 2.5:

$$\mu = \frac{\varepsilon_u}{\varepsilon_y} \tag{2.5}$$

Using structural steel has some disadvantages as well. Steel is usually considered an isotropic material. However, experimental data shows some anisotropic properties in terms of strength and ductility. Particularly, steel shows weakness in the perpendicular direction of lamination under tension stress. This phenomenon is called lamellar tearing. Fortunately, it is not significant in the majority of cases. It only must be taken into account in thick plates or heavy sections under deformation constrains caused by welding connections.

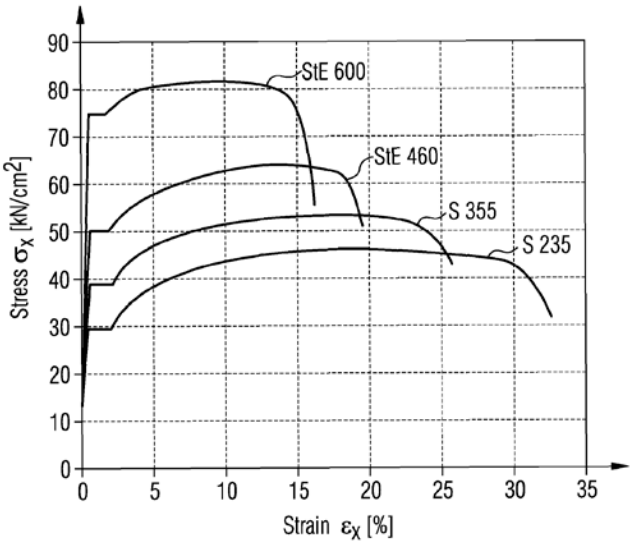

Figure 2.0.7. Stress-strain curves of S 235, S 355, StE 460 and StE E600. Rasmussen (2011)

Fatigue is another inherent problem in steel structures design and can play an important role in seismic response, specifically low cycle fatigue. Another significant drawback of structural steel is brittle fracture, which can produce failure even before reaching yield strength. In Figure 2.8 an example of brittle fracture after a seismic event can be observed. So, temperature must be taken into account too.

Residual stresses must not be forgotten. Finally, and perhaps the most important problem associated with structural steel is instability phenomena i.e. global buckling and local buckling. If all these disadvantages are considered and corrected by a good structure designer steel keeps being an excellent material for seismic design.

Steel is one of the most ductile materials used in structures. However, it would be a mistake to considerate that this property can be extrapolated automatically to the whole structural system. Buildings constructed with steel structures have been built during decades, mainly in developed countries. The earthquakes of Northridge, USA, in 1994 (Magnitude Richter 6,8) and Hyogo-ken Nanbu (Kobe), Japan, in 1995 (Magnitude Richter 7,2) represented a severe test for steel structures in this zones considered leaders in seismic engineering. No collapses in both earthquakes were recorded and the first inspections from the outside of the building indicated an adequate behavior with no observable damage with a plain sight. This situation was considered an engineering success of the steel industry. However, more detailed studies were carried out later and revealed that a significant number of buildings, most of them designed with modern standards, were seriously affected. Several weeks later specialized teams conducted inspections in order to investigate the occurrence of a important residual lateral displacement. For this purpose, they had to remove architectural elements and fire protection to see clearly the steel structure.

Figure 2.0.8. On the left: Fracture of a welded connection. On the right: Brace buckling, Earthquake of Hyogoken Nambu, Japan. Crisafulli (2012)

The most surprising and serious problems were reported in resistant moment frames (no braces), where it was observed an inadequate behavior of the connections, particularly in beam-to-column nodes. The type of failure was mainly the fracture of welds as can be seen in Figure 2.8 on the left. In Figure 2.9 a plate fracture can be observed.

Figure 2.0.9. Fracture in a base plate of a column of a braced frame caused by Northridge Earthquake. Crisafulli (2012)

The studies that were carried out concluded that the most important mistakes done in the metallic structure design and construction were:

- The use of inadequate electrodes in welding, which implies a low resilience values.
- Steel backing. It is useful for the welding process but is it a source of problems in the root of the weld.
- The presence of defects in the weld root that were not detected by ultrasound tests.
- The use of non-recommended construction practices like excessive heating of work pieces to increase the deposition rate of welding material.
- Other adverse effects, such as velocity effects of deformation (strain rate), interaction effects with reinforced concrete slabs, etc.

Brittle fractures took place in braced frames as can be seen in Figure 2.10. Buckling phenomena took place too as it can be observed in Figure 2.8 on the right.

Figure 2.0.10. Fracture of a brace and fracture of a welded connection. Crisafulli (2012)

Steel structures have evolved along more than one century. As a result of the experience and many investigations, some types and steel structure models have been developed to improve their behavior against seismic action. Here below these different types of steel structures are defined and commented.

2.1.5.1 Moment resisting frames (MRFs)

Moment resisting frames are composed of different components that form a resistant structure. Usually, their elements are rectilinear and arranged in a vertical and horizontal position (columns and beams). From the structural point of view the main components are beams, columns, beam-to-column connections, panel zones, column-to-column connections and column base plates. A schematic moment resisting frame with its components is shown in Figure 2.11.

This kind of frames tends to be translational and very ductile, dissipating a big amount of energy mainly in beams, which is useful in seismic zones. Even so, these frames are highly deformable structures, which can be a problem attending the serviceability limit state.

The different loads acting on the frame induce internal stresses, being the bending moment the main stress of design. The seismic action causes the maximum stresses at the end of the elements as it can be seen in Figure 2.11. That is why these zones are where the plastic hinges tend to appear. A plastic hinge is formed when a beam or column section reaches a certain value of moment, known as plastic moment. Plastic hinges allow rotation by keeping constant the resistant moment of the section.

Analytical and experimental considerations indicate that an excellent structural response can be achieved by designing “strong-columns-weak-beam”. This fact induces the generation of plastic hinges at the end of the beams while columns remain in the elastic range as it can be observed in Figure 2.12. Allowing the formation of plastic hinges in columns would jeopardize the global stability of the structure. The failure of a column could cause the building failure or an important part while the failure

of a beam would cause less significant damage. However there is an exception: plastic hinges appear in the base of some of the columns, as can be noted in Figure 2.12.

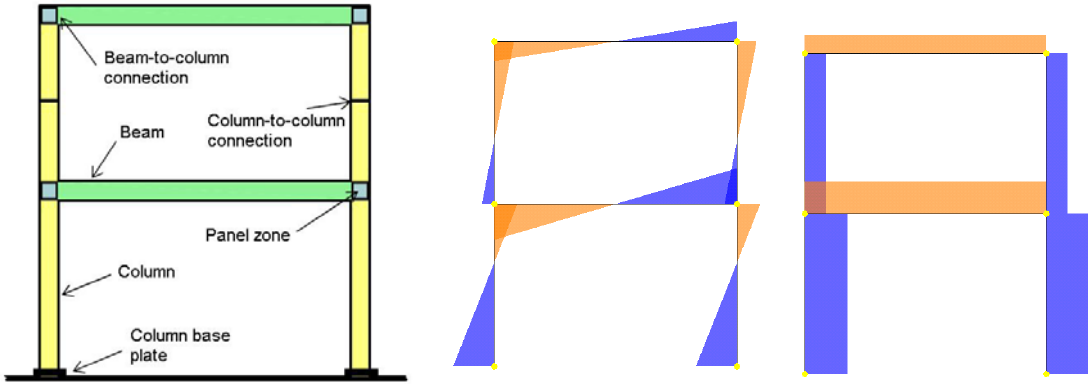

Figure 2.0.11. Moment resisting frames elements, bending moment and shear stress. Crisafulli (2012)

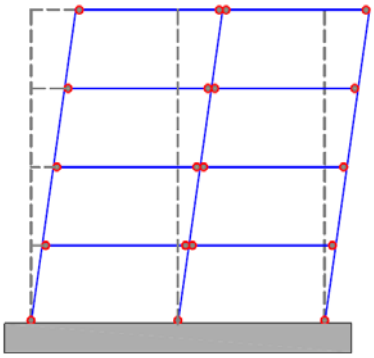

Figure 2.0.12. Plastic hinges in a moment resisting frame. Crisafulli (2012)

In order to assure that the plastic hinges are formed in beams, the following condition shown in Eq. 2.5 should be satisfied:

$$\frac{M_{c,Rd}\ (column)}{M_{c,Rd}(beam)} > 1 \qquad (2.5)$$

In Figure 2.13 are shown two different ways to make sure that the plastic hinge will appear in the beam and in the position desired by the structure designer. The solution in Figure 2.13 on the left is made by reducing the section at the flanges where the hinge is wanted to appear. And the solution in Figure 2.13 on the right is made by constructing very strong beam-to-column connection to assure the formation of the hinge just at the end of the connection.

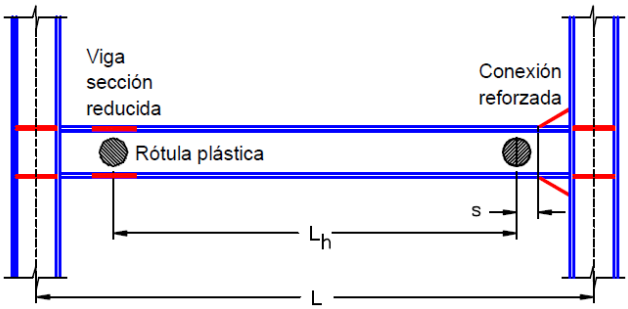

Figure 2.0.13. Position of plastic hinges. Crisafulli (2012)

2.1.5.2. Concentrically braced frames (CBFs)

The braced frames arose in the early twentieth century as a structural alternative for low and medium height buildings. The presence of the braces modifies the frame behavior significantly. Lateral actions like wind or seism induce on the structure tension and compression axial stresses because the structure has a cross-linked shape (with triangulations).

There are different configurations of concentrically braced frames as shown in Figure 2.14. The choice of the most suitable configuration for each case is made from structural considerations or functional as well. The choice is made from esthetical aspects eventually.

This structural type is characterized by a high lateral stiffness, which allows an adequate movement control. Furthermore, this kind of frame usually is intranslational, hence, it has less likeability to suffer buckling phenomena in beams and columns. However, its ductility is lower than for moment resisting frames. So, they have less ability to dissipate energy, braces can buckle and sometimes are an architectural inconvenient, although not always, as it can be seen in Figure 2.15 on the left.

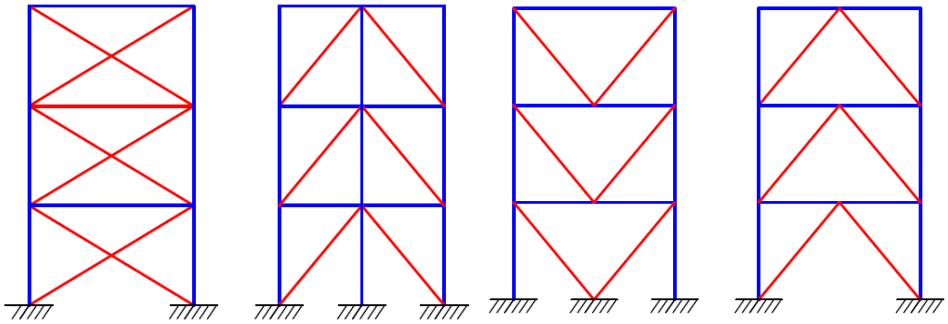

Figure 2.0.14. Concentrically braced frames. Crisafulli (2012)

Steel concentric braces have significant advantages for seismic rehabilitation. Steel components can be manufactured in the workshop and then assembled in the building with minimal alterations in its activity. Additionally, in certain cases, it is possible to put only steel braces to rehabilitate existing framed structures as shown in Figure 2.15 on the right.

Figure 2.0.15. On the left: “Hearst tower” in New York. On the right: steel braces of a rehabilitated concrete building. Crisafulli (2012)

Since the 1980s, seismic engineering developed different systems to improve the buildings seismic response. As it has been told, braces of frames can buckle, so, in order to improve this problem buckling constrained braces arose. This kind of braces dissipates energy by steel yielding avoiding their buckling. They can be changed easily in case of need after a seism. In Figure 2.16 buckling constrained braces are shown.

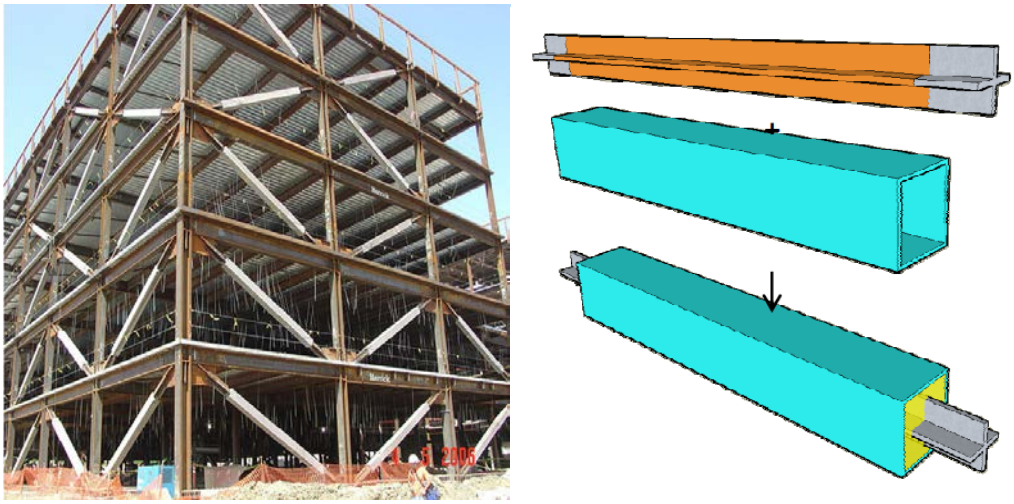

Figure 2.0.16. Buckling constrained braces. Crisafulli (2012)

2.1.5.3. Eccentrically braced frames (EBFs)

Moment resisting frames can exhibit a ductile and stable response, but they are relatively flexible structures and the design usually is limited by interstorey distortion or lateral displacement. Concentrically braced frames represent the opposite situation because are characterized by a high lateral stiffness, but their seismic behavior can be affected by the buckling of compressed braces. That is why in the 1970s, USA and Japan developed a new system that tried to combine the advantages of the previous two and counteract their weaknesses. Thus, the eccentrically braced frames emerged, whose braces are arranged deliberately generating an eccentricity in the beam, where

high shear stress and bending moment is induced. These zones are called links. In Figure 2.17 the most typical eccentrically braced frames schemes with its links in red are shown. Bending moment, shear and axial forces are shown in Figure 2.18.

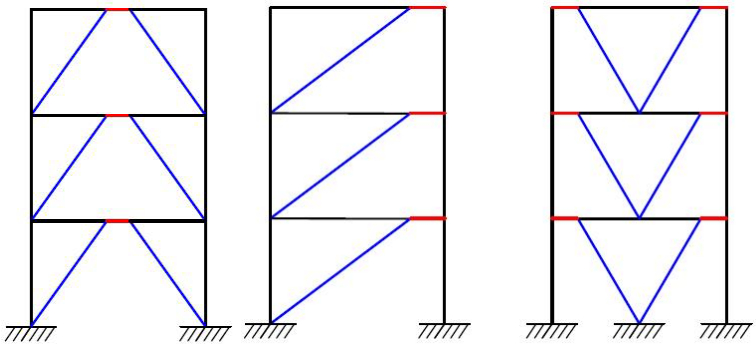

Figure 2.0.17. Eccentrically braced frames. Crisafulli (2012)

It is not advisable to generate a link in a column. It has already been told that is unwise to generate a plastic hinge in a column.

The braced frames with eccentric connections are a good example of the application of capacity design, through which the designer defines the mechanism of plastic deformations and prevents unwanted failure modes.

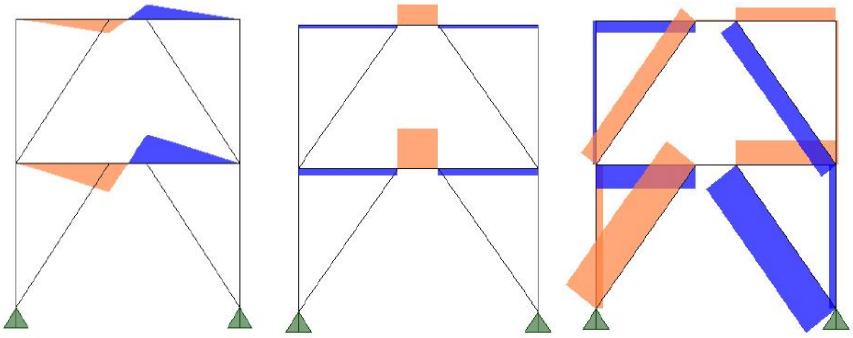

Figure 2.0.18. Bending moment, shear and axial force of a eccentrically braced frame. Crisafulli (2012)

These structures represent an excellent solution for the earthquake resistant design because they combine a high lateral stiffness, due to the braces, and a very adequate energy dissipation capability. For these reason, they were quickly adopted as a structural system from different types of earthquake resistant buildings, even in cases of rehabilitation of damaged structures.

2.1.6. Seismic standards

In this section some considerations regarding to different seismic standards are explained such as NCSE-02 (Spanish standard) and EN-1998 (European standard).

EN-1998 allows three methods to evaluate the seismic action: lateral force analysis, modal response spectrum analysis and non-linear methods like push-over analysis (non-linear static) or time-history analysis.

The fundamental period of vibration is one of the most important characteristics of a structure. Depending on the fundamental period, the seismic action can be amplified. So, it is one of the most important values to know to apply seismic standards.

Usually, the first step is to compute the first period or fundamental period of vibration of a structure and it can be obtained either by carrying out a modal analysis or by some simplified expressions given by standards.

Lateral force method

The lateral force method is applicable to those buildings whose response is not altered by vibration modes higher than fundamental period and when the Eq. 2.6 condition is met.

$$T_1 \leq \begin{cases} 4 \cdot T_C \\ 2\ s \end{cases} \tag{2.6}$$

Where T_1 is the fundamental period and T_C is the period related with the upper limit of the constant part of the spectral acceleration. T_C is represented in Figure 2.19. It must be noted that only the first period is used to take into account the seismic action.

This method cannot be used if the building is not regular along its height.

The first thing to do in the lateral force analysis is to calculate the base shear F_b, which is the total horizontal force applied to the structure. EN-1998 provides Eq. 2.7:

$$F_b = S_d(T_1) \cdot m \cdot \lambda \tag{2.7}$$

Where $S_d(T_1)$ is the ordinate of the spectrum for the fundamental period of the structure. The standard gives this expression of S_d and its graphic can be observed in Figure 2.19. m is the total mass of the building. And lambda is a correction factor for buildings with less than three storeys, in Eq. 2.8 lambda is described. The simplified formula that EN-1998 gives to compute the fundamental period for a moment resiting frame and for concentrically braced frames is shown in Eq. 2.9.

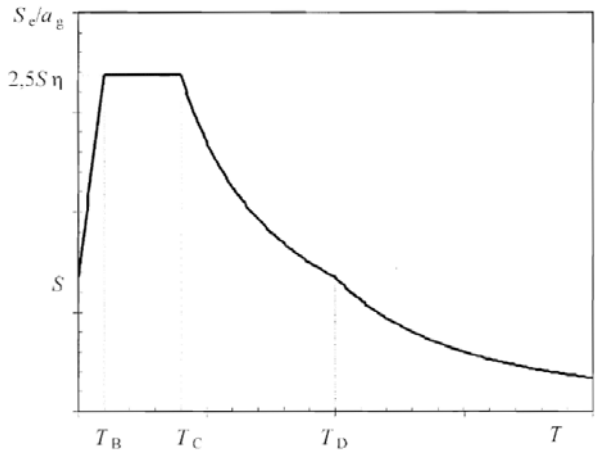

Figure 2.0.19. Elastic response spectrum of EN-1998 (2004)

$$\lambda = \begin{cases} 0{,}85 & \text{if } T_1 \leq 2T_C \quad \text{or} \quad \text{number of storeys} > 2 \\ 1 & \text{otherwise} \end{cases} \tag{2.8}$$

$$T_1 = C_1 H^{3/4} \quad \begin{cases} C_1 = 0{,}085 & for\ moment\ resisting\ frames \\ C_1 = 0{,}050 & for\ concentrically\ braced\ frames \end{cases} \tag{2.9}$$

Modal response method

The method of modal response spectrum should be applied in those buildings where it is not possible to apply the lateral force method.

All modes that contribute to the global response of the structure must be considered. So, EN-1998 impose that those modes whose sum of modal effective masses representing at least 90% of the weight of the structure must be taken into account. Every mode which represents an effective modal mass greater than 5% of the total mass has to be taken into account too.

For each modes the base shear is calculated analogously to the previous method as it shows Eq. 2.10.

$$F_{bk} = S_d(T_k) \cdot m_k \tag{2.10}$$

Once the base shear has been calculated, EN-1998 proposes two expressions to obtain the lateral forces. The first one is distribution depending on the fundamental period (Eq. 2.11) and the second one is a distribution making a lineal approximation (Eq. 2.12). In Figure 2.20 an explicative scheme is shown.

$$F_i = F_b \frac{s_i\, m_i}{\sum s_j\, m_j} \tag{2.11}$$

$$F_i = F_b \frac{z_i\, m_i}{\sum z_j\, m_j} \tag{2.12}$$

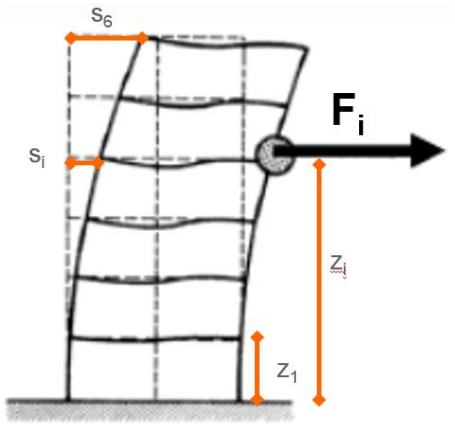

Figure 2.0.20. Lateral forces scheme

More precise methods like push-over analysis are allowed by EN-1998 (2004). It is a non-linear static analysis that keeps constant the gravitational loads while increases the horizontal ones monotonously with the aim of obtaining an overstrength ratio, estimating plastic mechanisms and damage distribution, and studying properly asymmetric buildings.

At least two vertical distributions of horizontal loads must be applied, an uniform one and another with the modal pattern shape. The result of this kind of analysis is a capacity curve, already explained in 2.1.4.2.

The most complex and complete method of calculation mentioned in the standard is the non-linear dynamic analysis, where the response of structures is obtained directly by integrating the differential equations of the movement. To perform this type of analysis is necessary to have adequate software, and the necessary knowledge to do so. The result is the roof displacement against time or other parameters like velocity, acceleration, stresses, etc.

NCSE-02 (Norma de construcción sismorresitente, Parte general y edificación), the Spanish standard, establishes as a reference for seismic analysis of the structure the response spectrums, based on modal analysis. Nonlinear dynamic analysis is allowed too.

Besides these two procedures the Spanish standard proposes a simplified method for the most common buildings. If the simplified method is wanted to be used, the building must meet the following characteristics:

- Less than twenty storeys
- Less than 60 meters high
- Geometric regularity in plan and elevation
- Continuity of columns to the foundation
- Regularity of stiffness, mass and strength in elevation
- Torsion eccentricity must not exceed 10%

This method can be used for residential buildings of normal importance with less than five storeys.

The standard imposes to evaluate three vibration modes excepting special cases, and to cut a long story short the following expressions (Eq. 2.13 and Eq. 2.14) allow to calculate the lateral forces to apply to the structure to represent the seismic action.

$$F_{ik} = s_{ik} P_k \tag{2.13}$$

$$s_{ik} = (a_c/g)\alpha_i \beta \eta_{ik} \tag{2.14}$$

Where P_k is the weight of storey k; a_c is the calculation acceleration given by the standard depending on the zone of the country; α_i is the value given by the response spectrum of the standard; β is a coefficient that takes into account the ductility of the structure and η_{ik} is the distribution factor for storey k and mode i obtained from the modal analysis.

2.2. Stainless steel

Stainless steel is a steel alloy that contains more than 10.5% of chromium which has excellent resistance to corrosion. The chromium content in mass ranges from 10.5% to 30% and the carbon content in mass is less than 1.2%. The addition of other metals to the alloy, such as molybdenum, titanium, niobium, manganese, nitrogen, copper, silicon, aluminum and vanadium, can improve its corrosion resistance and other physical properties.

Because of the chromium, steel allows the formation of an adherent and invisible corrosion resisting film on the steel surface. If this film is damaged mechanically or chemically, it heals itself, providing that oxygen, even in very small quantities, is present.

Because of its proprieties —hygiene, easy maintenance and durability— stainless steel became a reference for many applications like alimentary, automotive and medical industry. But its ability to blend easily with other materials has made stainless steel one of the most used materials by the construction industry actually. In Figure 2.21 different applications of stainless steel are shown.

Figure 2.0.21. Stainless steel uses (Arcelor-Mittal)

2.2.1. History

Stainless steel's use is relatively recent and it started to develop in 1920s. The alloy of iron and chromium was already used in 1821 but it was in 1904, in France, that Léon Guillet produced the first low carbon stainless steel. Few years later, in 1912, the first austenitic stainless steel was produced and patented by Eduard Maurer and Krupp. It was in 1913, in England, that Harry Brearley produced the first martensitic stainless steel trying to avoid the corrosion caused by alkaline food like lemon or vinegar.

In 1929, several American companies started to market stainless steel for applications in the building sector, such as lifts, entrance lobbies, façades, balustrades, door

frames, etc. They based their sales highlighting stainless steel's resistance to corrosion, its sanitary qualities and modern appearance. But it was in 1930s with the Chrysler Building (1930) and Empire State Building (1931) when stainless steel started to be promoted for architectural and construction issues. Chrysler Building is shown in Figure 2.21 on the left.

2.2.2. Life cycle cost: stainless steel's advantages

Stainless steel is often considered an expensive material when only the initial cost is taken into account. Following the current trend of considering lifecycle cost, operating costs (maintenance) and the residual value of the material should be considered too. In this case, stainless steel is presented as a competent material compared to others less resistant to corrosion as it can be seen in Figure 2.22.

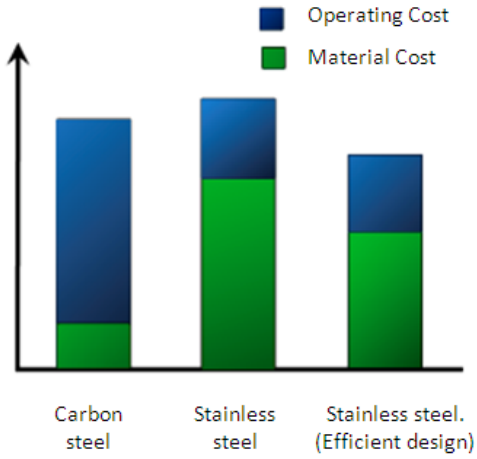

Figure 2.0.22. Comparison of the total costs between carbon steel and stainless Steel. Arrayago (2011)

2.2.3. The grades

There are more than one hundred grades of stainless steel. In European standard EN 10088 (2008) they are classified into seven main families -each of these has specific mechanical properties: hardness, yield stress, breaking strength, elongation, etc.- corresponding to precise metallurgical structures. In Figure 2.23 there is an explicative scheme of stainless steel grades according to their chemical components.

Here below some different families are described.

- Martensitic: 0.1% carbon, 10.5 to 17% chromium. Mainly used for tooling, cutting tools and springs.
- Ferritic: 0.02 to 0.06% carbon, 10.5 to 29% chromium, 0 to 4% molybdenum. These grades commonly used internally are now being developed for envelope and structural products. They offer excellent qualities for a cost price that is contained because of their low nickel content, material that suffers from highly speculative prices.
- Stabilised ferritic: with stabilizers, such as titanium, niobium or zirconium.

- Austenitic: 0.015 to 0.10% carbon, 16 to 18% chromium, 8 to 13% nickel, 0 to 4% molybdenum. The presence of nickel improves corrosion resistance and makes stainless steel more ductile. The presence of molybdenum further enhances the resistance to corrosion in an acid medium. Austenitic stainless steels account for 70% of global production.
- Stabilized austenitic: with stabilizers, such as titanium, niobium or zirconium.
- Low-nickel austenitic or “200 series”: these are chromium manganese steels, with low nickel content (always below 5%).
- Refractory austenitic: 0.2% maximum carbon, 20 to 25% chromium, 10 to 20% nickel.
- Austenoferritic (or “duplex”): with, for example: 0.02% carbon, 3% molybdenum, 5.5% nickel and 22% chromium. They have a two-phase austenite and ferrite structure. It has low content of nickel.

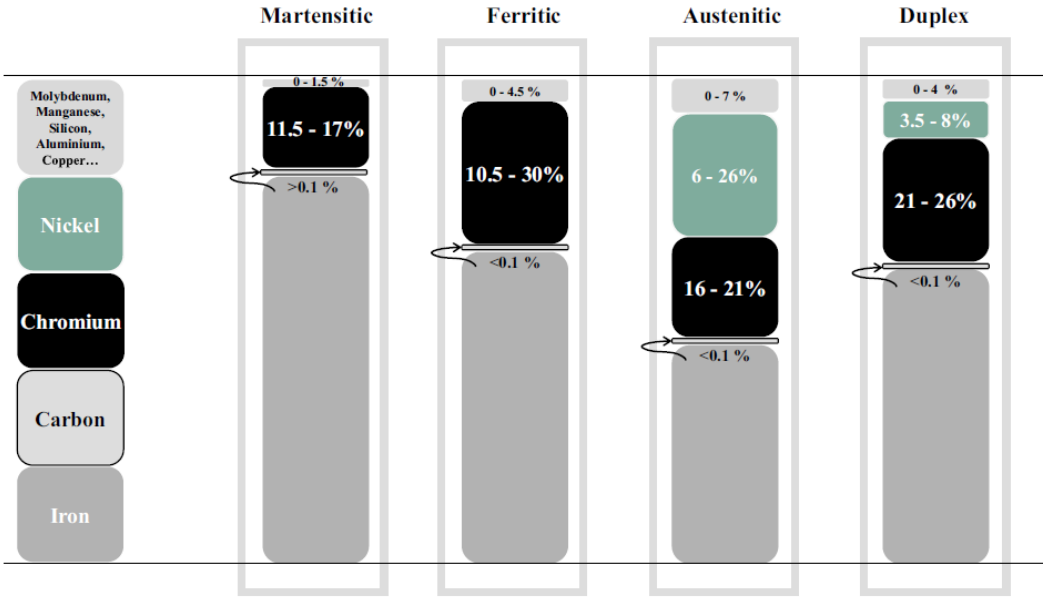

Figure 2.0.23. Indicative chemical composition depending on the family of stainless steel. Rossi (2014)

Although the high range of grades of stainless steel, not all of these are suitable for structural applications, particularly where welding is contemplated. In Figure 2.26 austenitic, ferritic and duplex stress-strain curves are shown. Austenitic, ferritic and duplex stainless steels are generally the more useful groups for structural applications, Figure 2.24 becomes very explicative. Austenitic stainless steels provide a good combination of corrosion resistance, forming and fabrication properties. Duplex stainless steels have high strength and wear resistance with very good resistance to stress corrosion cracking. Ferritic stainless steels have better mechanical properties than austenitic ones, and they are cheaper and price-stable because of their low content of nickel.

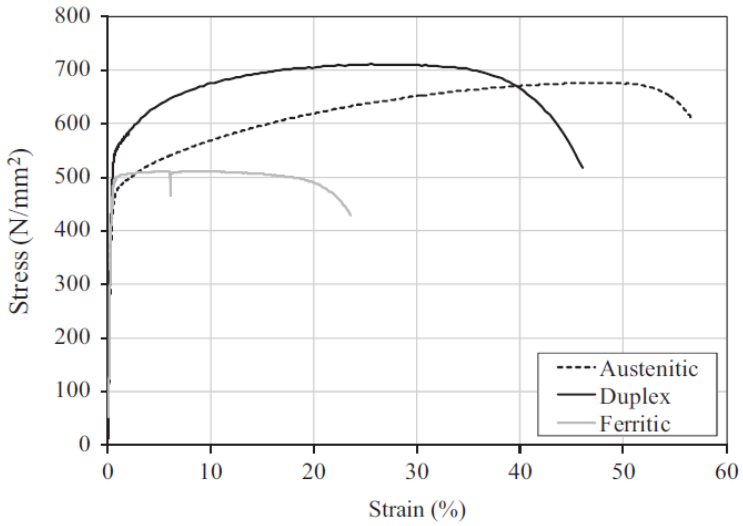

Figure 2.0.24. Typical stress-strain curves for austenitic, duplex and ferritic stainless Steel. Rossi (2014)

2.2.4. Names

Stainless steel names are designated according to EN 10088 (2008) with a number and a name designation which also includes the composition. In Figure 2.25 one stainless steel is shown with its name according to EN 10088.

1.	**43**	**07**
Denotes steel	Denotes one group of stainless steel	Individual grade identification

X	**2**	**CrNi**	**18-9**
Denotes high alloy steel	100x % of carbon	Chemical Symbols of main alloying elements	% of main alloying elements

Figure 2.0.25. Stainless steel nomenclature according to EN 10088 (2008)

In Table 2.1 there are the most common stainless steels with their main mechanical properties.

	Grade	Product form[1]	Max thickness (mm)	Minimum 0.2% proof strength[2] (N/mm^2)	Ultimate tensile strength (N/mm^2)	Elongation after fracture (%)
Basic chromium-nickel austenitic steels	1.4301	C	8	230	540 – 750	45[3]
		H	13,5	210	520 – 720	45[3]
		P	75	210	520 – 720	45
	1.4307	C	8	220	520 –700	45
		H	13,5	200	520 –700	45
		P	75	200	500 – 700	45
Molybdenum-chromium-nickel austenitic steels	1.4401	C	8	240	530 – 680	40
		H	13,5	220	530 – 680	40
		P	75	220	520 – 670	45
	1.4404	C	8	240	530 – 680	40
		H	13,5	220	530 – 680	40
		P	75	220	520 – 670	45
Stabilised austenitic steels	1.4541	C	8	220	520 – 720	40
		H	13,5	200	520 – 720	40
		P	75	200	500 – 700	40
	1.4571	C	8	240	540 – 690	40
		H	13,5	220	540 – 690	40
		P	75	220	520 – 670	40
Low carbon, high nitrogen austenitic steel	1.4318	C	8	350	650 – 850	35
		H	13,5	330	650 – 850	35
		P	75	330	630 – 830	45
Duplex steels	1.4362	C	8	450	650 – 850	20
		H	13,5	400	650 – 850	20
		P	75	400	630 – 800	25
	1.4462	C	8	500	700 – 950	20
		H	13,5	460	700 – 950	25
		P	75	460	640 – 840	25

Notes:
(1) C = cold rolled strip, H = hot rolled strip, P = hot rolled plate
(2) Transverse properties
(3) For stretcher levelled material, the minimum value is 5% lower

Table 2.0.1. Specified mechanical properties of common stainless steels according to EN 10088 (2008)

2.2.5. Properties

Every single grade of stainless steel has different qualities, such as its ability to resist corrosion in aggressive environments, temperatures, absorb impacts, etc. That is why the various grades of stainless steel constitute a family of materials likely to answer a broad variety of potential requests. The choice of the suitable grade for the environment where the stainless steel will be placed (chemical, maritime, etc) is best left to the designers.

Stainless steel is not only an interesting material for its corrosion resistance but also for its mechanical strength (550 to 1400 MPa), its yield stress (220 to 1100 MPa) and its extremely favorable ratio of Young's modulus of elasticity to density. That makes this material ideal for structures like footbridges and construction in seismic zones because combines stiffness with light weight. It also has other appreciated qualities, such as fire resistance, strength and ductility at very low temperatures, durability, recyclability and aesthetics.

The main difference between stainless steels and carbon steels is the shape of strain-stress curves. Carbon steel shows a linear behavior until its yield point and a flat area before hardening. On the other hand, stainless steels have a more rounded response and show a non-linear behavior from small load levels without a clearly defined yield point. Therefore, stainless steel "yield" strengths are generally quoted in terms of a proof stress defined for a particular offset permanent strain, conventionally the 0,2% plastic strain. Figure 2.26 shows typical experimental stress-strain curves for carbon steel and some different stainless steel.

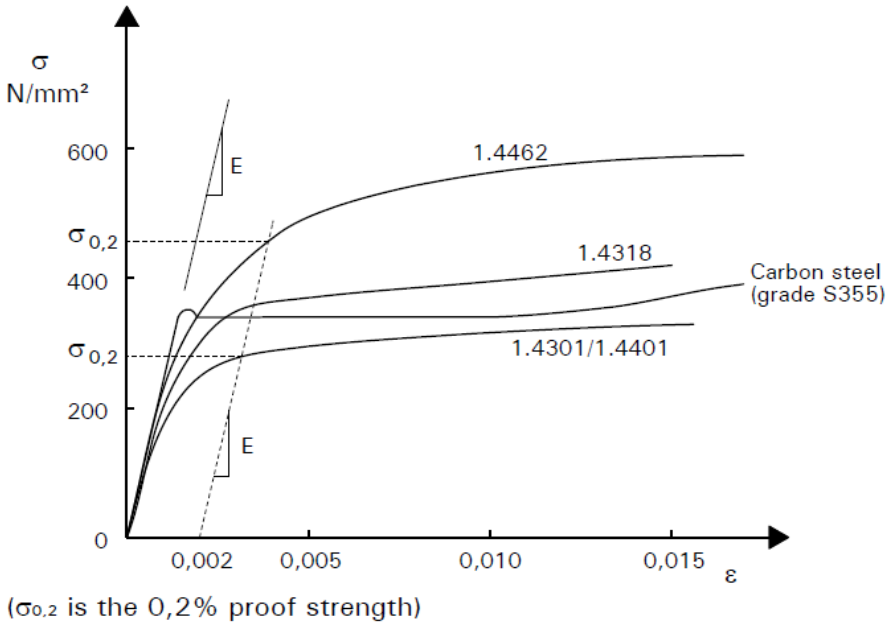

Figure 2.0.26. Typical stress-strain curves for stainless steel and carbon steel. Design Manual for Structural Stainless Steel (2006)

There are some factors that can change the shape of the basic stress-strain curve for any given grade of stainless steel, for example:

- Cold working: Strength levels are enhanced by cold working. Associated with this enhancement, a reduction in ductility is noted, but this normally has no consequences due to the initial high values of ductility, especially for the austenitic stainless steels.
- Strain-rate sensitivity: A proportionally greater strength can be performed at fast strain rates for stainless steel than for carbon steel.
- Heat treatment: Annealing, or softening, reduces the strength enhancement and the anisotropy.

Thanks to these properties stainless steel is available in many different forms. Cold formed products such as plates, sheets, coils, strips (in thicknesses typically ≤ 6,0 mm), round bars (diameters from 5 mm to 60 mm), square and rectangular hollow sections (cross-section dimensions up to 400 mm, thicknesses from 1.2 to 6 mm) can be easily obtained.

Another interesting property of stainless steel is the amount of possibilities to finishes its surface. Sometimes, in certain applications, surface finish and appearance is important. Manufacturers offer a wide range of standard finishes, from mill finish through dull finishes to bright polish. Although the various finishes are standardized, variability in processing introduces differences in appearance between manufacturers and even from a single producer.

Bright finishes are frequently used in architectural applications and it should be noted that bright finishes will exaggerate any out-of-flatness of the material, particularly on panel surfaces. Stiffened, embossed, textured, patterned or profiled sheets with a rigid supporting frame will reduce this tendency.

3. ANALYSIS TYPES AND MODAL CALIBRATION

An introduction of the analysis types and the calibration that has been made to assure confident results are explained in this section.

3.1. Introduction

3.1.1. Software

The software used to compute the different analysis cases in this study has been SAP2000. This software was developed by CSI, Computer and Structures, Inc. Berkeley, California, USA. It has been in continuous development during more than 30 years to give to the engineer a reliable, sophisticated and easy to use tool. It has a powerful and intuitive graphical interface of modeling procedures and structural analysis and design. It is one of the most forefront programs in the world of structural calculations.

In terms of usage it allows various static and dynamic types of analysis: linear or non-linear from spectral or time-history functions. In the calculations different structural components such as wires, dampers or non-prismatic sections can be incorporated.

SAP2000 determines by the finite element method the response in terms of forces, stresses and deformed shape the area or solid elements, presenting a graph and output tables, making it useful for structural engineers engaged in research or construction and project managers.

In relation to non-linear analysis, capacity curves can be obtained by the application of a push-over analysis and by defining plastic hinges at the end of the elements. These capacity curves allow studying failure mechanisms of the model of study, obtaining its ductility, overstrength, ultimate strength, inelastic deformation, etc.

Additionally, the hinges performance is computed following the criteria of FEMA 356 Standards, FEMA 440 and ATC 40. This allows validating the normative procedures in the area of seismic design.

Moreover, SAP2000 can obtain the critical buckling load for systems of lines, for example, for steel beams. It also can run modal analysis to obtain the periods of vibration of the structures.

3.1.2. Modal analysis

The main aim of the modal analysis is to obtain the periods of vibration of a structure. So, it is needed to know the conditions of equilibrium of moment frame buildings that are shown in matrix form in Eq. 3.1.

$$\mathbf{F}_{\mathrm{i}}(\mathrm{t}) - \mathbf{F}_{\mathrm{e}}(\mathrm{t}) - \mathbf{F}_{\mathrm{a}}(\mathrm{t}) = 0 \qquad (3.1)$$

Where $\mathbf{F}_{\mathrm{i}}(\mathrm{t})$ is the vector of inertial forces, $\mathbf{F}_{\mathrm{e}}(\mathrm{t})$ is the vector of elastic forces and $\mathbf{F}_{\mathrm{a}}(\mathrm{t})$ is the vector of dumping forces and are defined in Eq. 3.2, Eq. 3.3 and Eq. 3.4.

$$\mathbf{F}_{\mathrm{e}}(\mathrm{t}) = \mathbf{K}\mathbf{U}(t) \tag{3.2}$$

$$\mathbf{F}_{\mathrm{i}}(\mathrm{t}) = -\mathbf{M}\left[\ddot{\mathbf{U}}(t) + \{1\}a(t)\right] \tag{3.3}$$

$$\mathbf{F}_{\mathrm{a}}(\mathrm{t}) = \mathbf{C}\dot{\mathbf{U}}(t) \tag{3.4}$$

Where $\mathbf{U}(\mathrm{t})$ is the displacements vector; $\{1\}$ is the position vector of the accelerations; $\mathbf{K}$ is the stiffness matrix and $\mathbf{M}$ is the mass matrix.

Then, by replacing Eq. 3.2, Eq. 3.3 and Eq. 3.4 in Eq. 3.1, Eq. 3.5 is obtained.

$$\mathbf{M}\ddot{\mathbf{U}}(t) + \mathbf{C}\dot{\mathbf{U}}(t) + \mathbf{K}\mathbf{U}(t) = -\mathbf{M}\{1\}a(t) \tag{3.5}$$

The damped free vibrations in the dynamic model are expressed like:

$$\mathbf{M}\ddot{\mathbf{U}} + \mathbf{C}\dot{\mathbf{U}} + \mathbf{K}\mathbf{U} = 0 \tag{3.6}$$

And if the dumping effect is ignored:

$$\mathbf{M}\ddot{\mathbf{U}} + \mathbf{K}\mathbf{U} = 0 \tag{3.7}$$

The dynamic characteristics of the models with multiple degrees of freedom are defined by its non-damped free vibrations, defined by Eq. 3.7. This equation must be true for particular solutions of the type

$$\mathbf{U}(\mathrm{t}) = \varphi e^{iwt} \tag{3.8}$$

Vector φ contains displacement amplitudes and w is the pulsation. Hence, from Eq. 3.7 and Eq. 3.8, Eq. 3.9 is obtained.

$$(\mathbf{K} - \mathrm{w}^2\mathbf{M})\varphi = \mathbf{0} \tag{3.9}$$

This system of linear algebraic and homogeneous equations constitutes an eigenvector problem and its non-trivial solutions, the eigenvalues (w_i^2), are the different pulsations square. Hence, the periods can be easily obtained.

$$T_i = \frac{2\pi}{w_i} \tag{3.10}$$

The greatest value of T_i is the fundamental period, T_1. The eigenvectors, for example, φ_{i1}, represents the modal shape of the period T_1.

The eigenvectors can be normalized by different manners, but the most common one for buildings is to normalize them by the total mass as it is shown in Eq. 3.11 and Eq. 3.12.

$$\varphi_i^T \boldsymbol{M} \varphi_i = M_i^* \tag{3.11}$$

$$\phi_i = \varphi_i (M_i^*)^{-1/2}, \quad i = 1,2,\dots n \tag{3.12}$$

3.1.3. Push-over analysis

As it has already been commented, the push-over analysis is a non-linear static analysis that keeps constant the gravitational loads while increases the horizontal ones monotonously in order to obtain capacity curves. It is needed to define plastic hinges at the end of the elements to perform the inelastic response of the structure.

FEMA, the Federal Emergency Management Agency and ASCE, American Society of Civil Engineers, after the Northridge earthquake in 1994, began to develop and change the edification codes where new connection types were proposed to improve the performance against the seismic action. Plastic hinges were defined too. The plastic hinges that are used in SAP2000 are gathered in FEMA 356 (2000), FEMA 440 (2005) and ATC 40 (1996). Specifically, steel hinges are defined in FEMA 356, chapter 5. In Figure 3.1 the hinges behavior is shown.

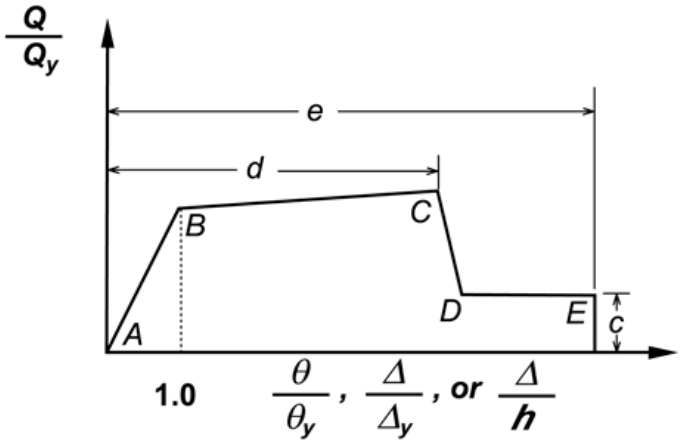

Figure 3.1. Generalized force-deformation relation for steel elements or components. FEMA 356 (2000)

Parameters e, d, and c are also specified in FEMA 356 tables. Modification of this curve is allowed to account for strain-hardening of components if there are experimental data available. The parameters Q and Q_{CE} in Figure 3.1 are the generalized component load and the generalized component expected strength, respectively. For beams and columns, θ is the total elastic and plastic rotation of the beam or column, θ_y is the rotation at yield, Δ is the total elastic and plastic displacement, and Δ_y is the yield displacement.

FEMA 356 also defined different parts of the graphic shown in Figure 3.1. These parts gave to the engineer the safety level of each hinge as it can be seen in Figure 3.2.

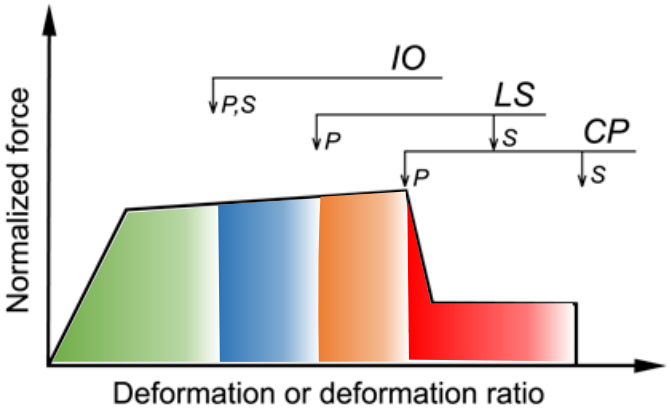

Figure 3.2. Component or element deformation acceptance criteria. FEMA 356 (2000)

So, this graphic shows the acceptance criteria for deformation or deformation ratios for primary members (P) and secondary members (S). The area in red corresponds to failure, the area in orange corresponds to the Collapse Prevention level (CP), the area in blue corresponds to Life Safety level (LS) and the area in green corresponds to the Immediate Occupancy level (IO).

The calculations made with SAP2000 show the state of every hinge for each step of incremental force and it is possible to see in which portion of the graphic in Figure 3.2 the hinge is. So, push-over analysis allows the knowledge of the evolution of hinges formation and the evolution of the safety level of the structure.

3.2. Calibration

Usually, experimental tests are very expensive, particularly when it is wanted to test an entire building under a seismic action. Therefore, numerical modeling is very useful as it allows a reliably reproduction of the reality and performs tests quickly and cheaply. However, it is necessary as a first step to verify that the model that is going to be used in the analysis is in effect representing properly the reality by calibrating it. Calibration is carried out by confirming that the results obtained by the model of the study are similar to others that have been proved as reliable ones. So, this model is used as a benchmark.

The structure used to calibrate the model obtained from Di Sarno and Nethercot (2003) and the results of the calibration are shown in this section. This model was made in carbon steel and stainless steel. That is why it has been the chosen one.

3.2.1. Model

A moment resisting frame has been used for the model calibration. It has three spans and six storeys. External spans have 8 m and the internal span has 6 m. It has been considered that the distance between the adjacent frames is 5 m.

It is an office building. So, storeys are slightly higher than if it was a residence building. The first storey has 4,5 m of height and the rest are 3,5 m high and as a result, the whole building is 22 m high. A scheme of the calibration model is shown in Figure 3.3.

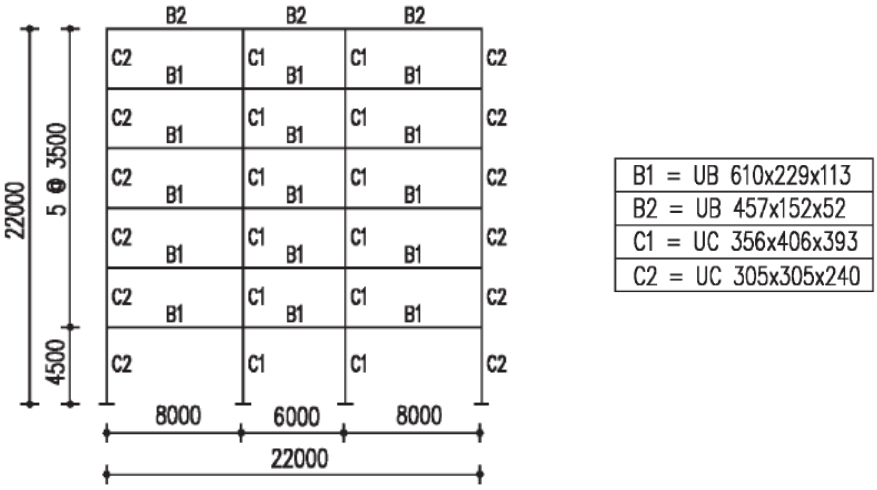

Figure 3.3. Calibration model scheme

This scheme shows that the internal columns are stronger than the external ones such as the beams of the roof are weaker than the beams of the other storeys as well. Beams and columns cross sections are described in Figure 3.4 and in Table 3.1. These kinds of cross sections are mostly used in countries of the Commonwealth.

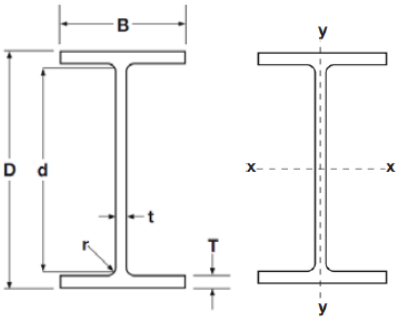

Figure 3.4. Definition of the symbols in Universal beams and columns cross-sections

	W	D	B	t	T	r	d	Ix	Iy
	Kg/m	mm	mm	mm	mm	mm	mm	cm^4	cm^4
UB									
610x229x113	113	607,6	228,2	11,1	17,3	12,7	547,6	87320	3434
457x152x52	52,3	449,8	152,4	7,6	10,9	10,2	407,6	21370	645
UC									
356x406x393	393	419	407	30,6	49,2	15,2	290,2	146600	55370
305x305x240	240	352,5	318,4	23	37,7	15,2	246,7	64200	20310

Table 3.1. Cross section measures and moments of inertia

In the model has been considered each storey as a rigid diaphragm of concrete slabs with a depth of 150 mm for floors and 120 mm for the roof. These slabs do not contribute significantly to the flexural strength of the beams. This fact means that the relative movement along every floor is restrained.

It is assumed that lateral torsional buckling is avoid by secondary members. Furthermore, it is also assumed that panel distortion in columns and web instability in beams are prevented by adequate stiffeners.

Moreover, this frame has been designed in compliance with European standards for static and dynamic loading. It has also been checked by US seismic standards and provisions, for instance, cross section width-to-thickness slenderness limitations or column-to-beam moment ratios.

Overstrength requirements are accomplished by using full penetration welds. The inertia of the columns is greater than the beams assuring this way the hinge formation in the beams (strong-column-weak-beam).

Carbon steel and stainless steel grades have been chosen conscientiously to allow an easy comparison between their behaviors. So, for this purpose both materials have the same yielding and proof stress, f_y=275 N/mm^2. For carbon steel, f_u/f_y ratio is 1,59 and for stainless steel is 2,00. The ultimate strain assigned to stainless steel is 50% while the assigned to carbon steel is 25%.

SAP2000 does not allow to compute capacity curves with non-linear materials such as stainless-steel. To solve this problem stainless steel has been defined as a carbon steel but with its ultimate stress and strain. In Figure 3.5 can be seen the stress-strain curves for each material defined in SAP2000.

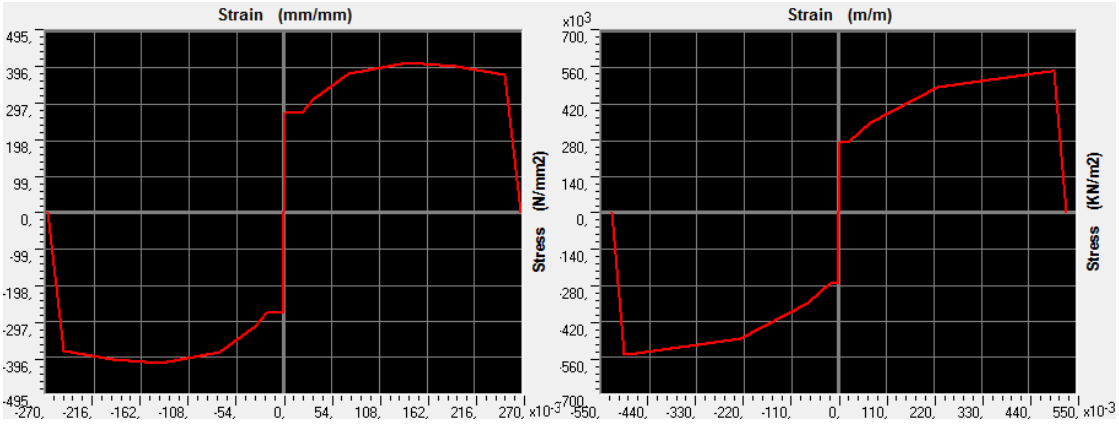

Figure 3.5. Stress-strain curves modeled with SAP2000, carbon steel (left), stainless steel (right)

Other structural schemes have been used to calibrate the model in the modal analysis and they are shown in Figure 3.6 and Figure 3.7. These models have been obtained from Di Sarno and Nethercot (2003) too.

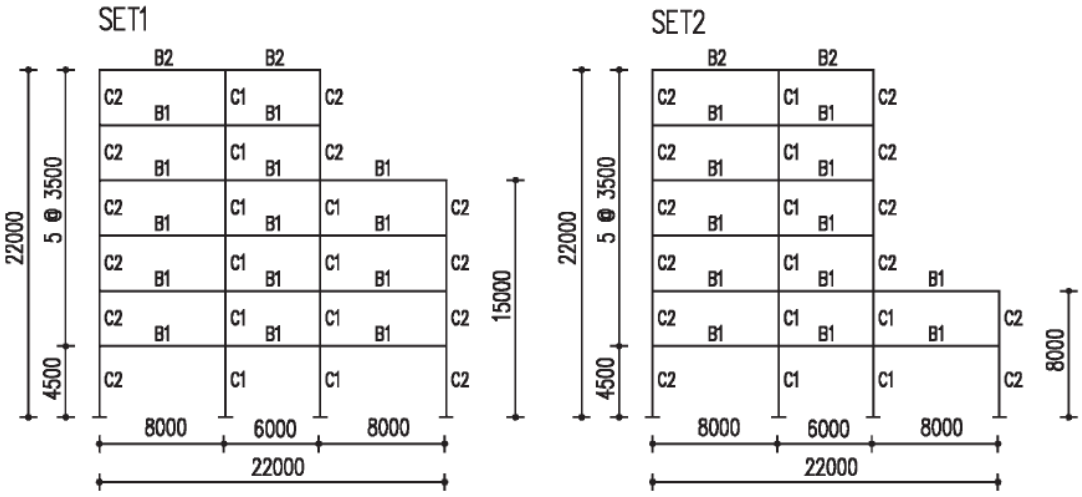

Figure 3.6. SET1 and SET2

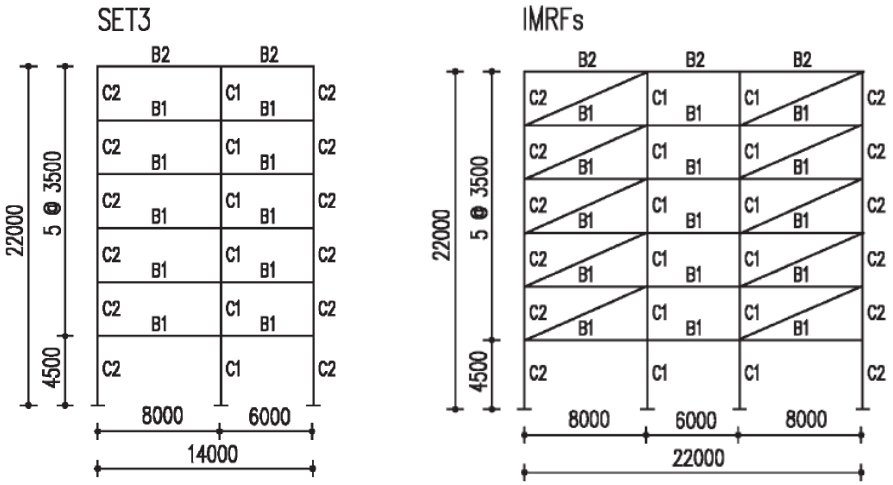

Figure 3.7. SET3 and IMRF

3.2.2. Calibration

The resisting moment frame described in 3.2.1. is the same used for Di Sarno and Nethercot (2003) with the purpose of use their results as a benchmark. Hence, in order to assure confident results, the calculations of this study have been compared with the ones made by them.

A modal analysis and a pushover analysis have been carried out. The fundamental periods obtained by the modal analysis, the benchmark results and the results given by the EN-1998 formula are shown in the Table 3.2.

	T (EN-1998) s	T (Benchmark) s	T (Calibration) s	T_C/T_B
RMRF	0,86	0,94	0,93	0,99
IMRF	0,86	0,56	0,59	1,05
SET1	0,86	0,85	0,85	0,99
SET2	0,86	0,83	0,82	0,99
SET3	0,86	0,91	0,91	1,00
Mean	-	-	-	**1,01**
Cov	-	-	-	**0,024**

Table 3.2. Fundamental period calibration

From the results shown in Table 3.2 can be concluded that the results of the calibration are satisfactorily confident.

Regarding to the pushover analysis, shear deformation has been taken into account. Second order effects such as P-Δ has been considered as well. Panel zones strength and deformations and the additional strength of the concrete slabs have not been taken into account. The hinges assigned at the end of the elements not only take into account the bending moment but the axil force too. These hinges properties are gathered in FEMA-356 and explained in this work in section 3.1.3.

The pushover horizontal force distribution is triangular.

The comparison between the capacity curves obtained in this study and the benchmark are shown in Figure 3.8.

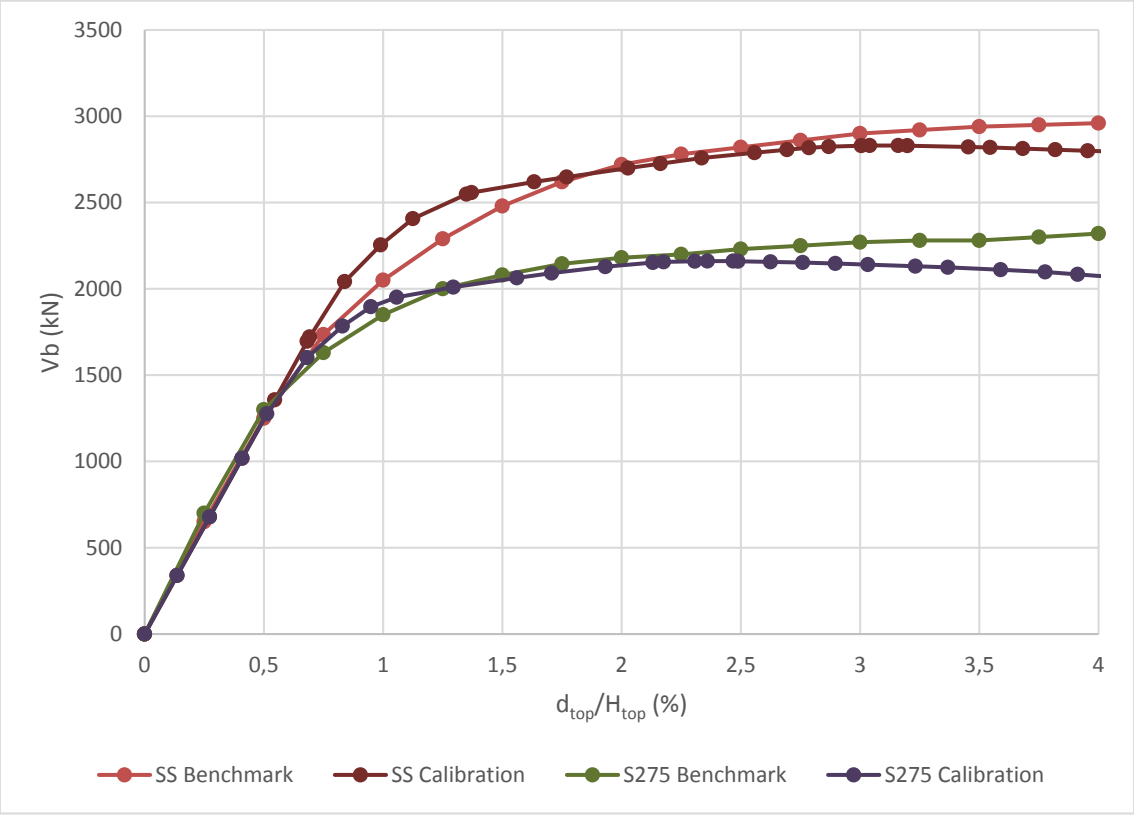

Figure 3.8. Capacity curve calibration

As it can be observed, the results are similar, but the capacity curves of the benchmark do not decrease while the calibration capacity curves do. The point where the capacity curve start to decrease is the point where the structure collapse. The benchmark capacity curves show an infinite hardening, which it has no sense physically, but they solved this problem by defining a failure point with another method. In this study, the failure point is obtained by finding the point where the capacity curve starts to decrease. Numerically, the results are similar, so it can be deducted that the capacity curves of this study will be reliable.

Although the results are acceptable, it must be aware of the limitations of the calculations made with SAP2000, specifically with the stainless steel definition. Stainless steel has a rounded transition between the elastic and the plastic part of its stress-strain curve. And as it has already shown in Figure 3.5 stainless steel has been modeled as a more ductile carbon steel. This fact makes understandable the difference between the calibration capacity curve and the benchmark one, specifically when the structure starts to yield. The calibration curve shows almost a bilinear behavior while the benchmark one shows a rounded transition when yielding begins.

However, these differences are not important because in the linear and in the plastic portion of the curve the results are very close to the benchmark. Furthermore, the aim of this study is to evaluate the differences between the seismic behavior of these two materials, where the collapse of the structures is analyzed. Hence, the ultimate properties of the material, such as ductility, ultimate elongation and ultimate strength are the ones defining the ultimate response of the structure. Summarizing, the main factors of interest when an earthquake takes place.

4. CASE OF STUDY

The results obtained from the study cases are shown and explained in this section. The analysis of the results is shown as well.

4.1. Definition of the models

Two different frames have been chosen to compute the analysis and evaluate the influence of including stainless steel elements to different types of frames in order to obtain a better seismic performance of the structures. Both have the same general dimensions of the RMRF (Regular Moment Resisting Frame) introduced as the calibration model. In fact, the only difference between the RMRF of the calibration and the RMRF of the case of study is the cross-section definition of the beams and columns. The two cases of study, a RMRF and a CBF (Concentrically Braced Frame) are shown in Figure 4.1 and Figure 4.2 respectively, showing the general dimensions of the frames and the definition of cross-sections for beams, columns and braces.

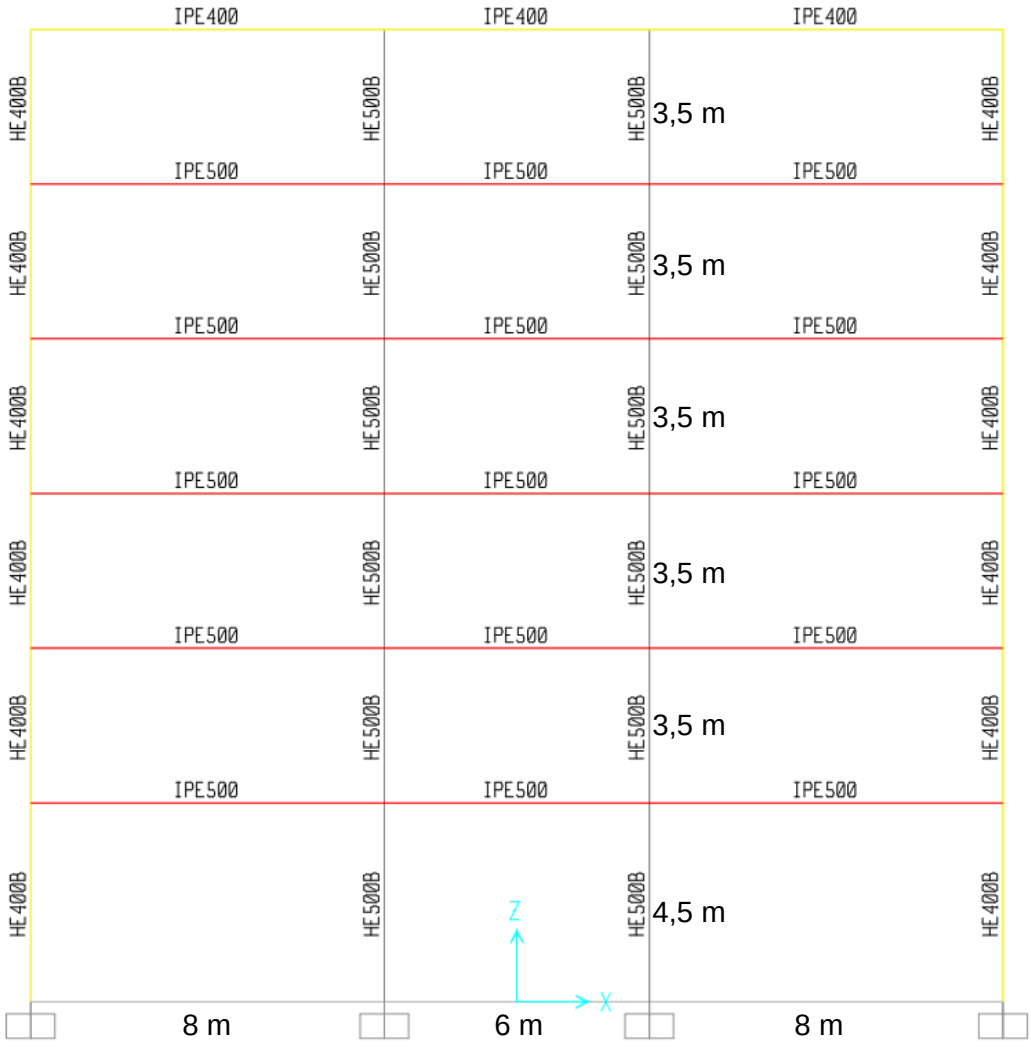

Figure 4.1. RMRF of study

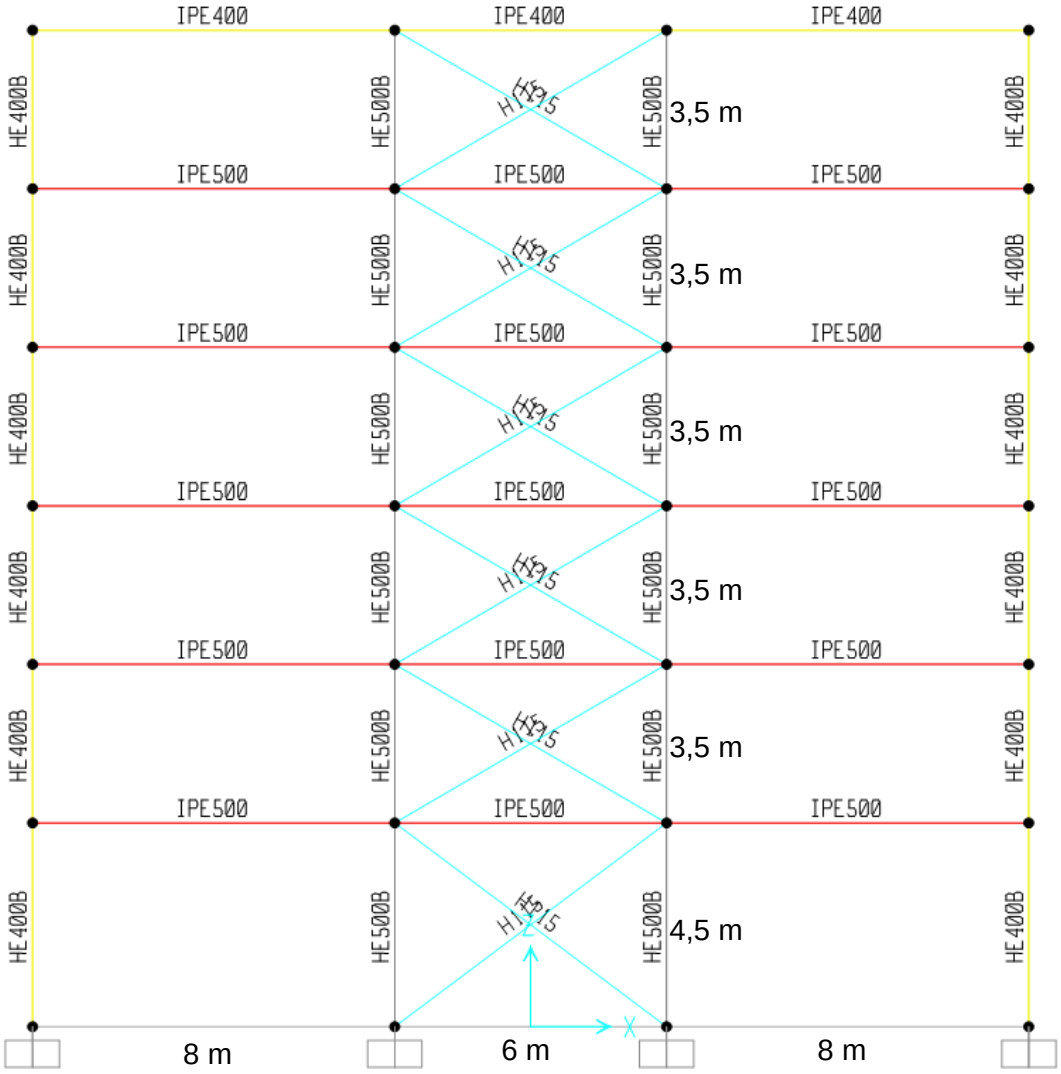

Figure 4.2. CBF of study

As it can be seen, the cross-sections are the European ones. The braces have been defined as circular hollow sections with an external diameter of 115 mm and 4mm of thickness. These braces have the local and general buckling restrained, what could be achieved by filling the hollow section with concrete or by other methods that are not of interest in this work. All the structural hypothesis made in 3.1.2 are valid for the model calculations, being the main ones that it has been considered each storey as a rigid diaphragm, it is assumed that lateral torsional buckling is avoid by secondary members and it is also assumed that panel distortion in columns and web instability in beams are prevented by the adequate stiffeners. In Figure 4.3 the description of the cross-sections is shown. The dimensions and the second moments of area of the cross-sections defined in the cases of study are shown in Table 4.1.

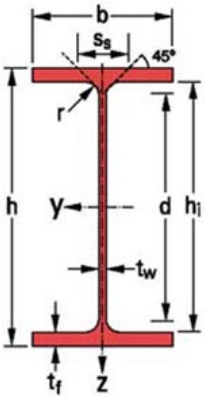

Figure 4.3. Definition of the symbols in the European beams and columns cross-sections

	W	h	b	t_w	t_f	r	d	Iy	Iz
	Kg/m	mm	mm	mm	mm	mm	mm	cm^4	cm^4
Beams									
IPE500	90,7	500	200	10,2	16	21	426	48202	2142
IPE400	66,3	400	180	8,6	13,5	21,	331	23131	1318
Columns									
HEB500	187,3	500	300	14,5	28	27	390	107181	12624
HEB400	155,3	400	300	13,5	24	27	298	57684	10819

Table 4.1. Cross-section measures and second moments of area

The materials of the frames analyzed in this section are the same to the ones defined for the calibration models, i.e. S275 and a stainless steel with a yielding stress of 275 N/mm^2. For carbon steel, f_u/f_y ratio is 1,59 and for stainless steel is 2,00. Stainless steel has higher values of f_u and especially of ε_u than carbon steel for the same yielding stress. From this stainless steel property arose the motivation of doing this study.

4.2. Results: capacity curves for different structural and material configuration

The first calculations made in this study have been the capacity curves of the frames with all their members of carbon steel. These results have been considered as a benchmark for the other cases of study, so increments in ultimate basal loads and deformations will be refered to the values obtained for this case. After obtaining these benchmark curves, it has been conducted an analysis by changing the material of the elements of the frames from carbon steel (S275) to stainless steel in order to determine where the use of stainless steel improves more effectively the global response of the frame against the seismic action.

The nomenclature used in the cases of study is explained with the following example: case CBF-C-S-C, meaning concentric braced frame (CBF) with the columns of carbon steel (C), stainless steel beams (S) and carbon steel braces (C). The cases of study with the materials used in each element type are shown in Table 4.2. CS means carbon steel and SS means stainless steel.

	Columns	Beams	Braces
RMRF-C-C	CS	CS	-
RMRF-S-S	SS	SS	-
RMRF-C-S	CS	SS	-
RMRF-S-C	SS	CS	-
CBF-C-C-C	CS	CS	CS
CBF-S-S-S	SS	SS	SS
CBF-C-C-S	CS	CS	SS
CBF-C-S-C	CS	SS	CS
CBF-S-C-C	SS	CS	CS
CBF-C-S-S	CS	SS	SS
CBF-S-C-S	SS	CS	SS
CBF-S-S-C	SS	SS	CS

Table 4.2. Materials of the cases of study

12 modal and pushover analyses have been carried out in this present study. This has been conducted by combining carbon and stainless steel materials in the different members of the frames as shown in Table 4.2 (beams, columns and braces) in order to know where the stainless steel proprieties are more advantageous for the seismic action.

The fundamental period of the RMRF is 1,15 s and the CBF on is 0,74 s, which does not vary when changing materials, as both considered materials show the same Young's modulus and yield stress values. Obviously, the fundamental period of the CBF is lower than the RMRF. That is why the braces make the CBF a much more rigid frame than the RMRF that it has not braces, what considerably reduces the fundamental period.

4.2.1. RMRF

In this section, the hinge formation evolution, the capacity curves of RMRFs and their main values of the capacity curves are presented in this order.

First of all, in Figure 4.4 the hinge formation evolution of RMRF is shown.

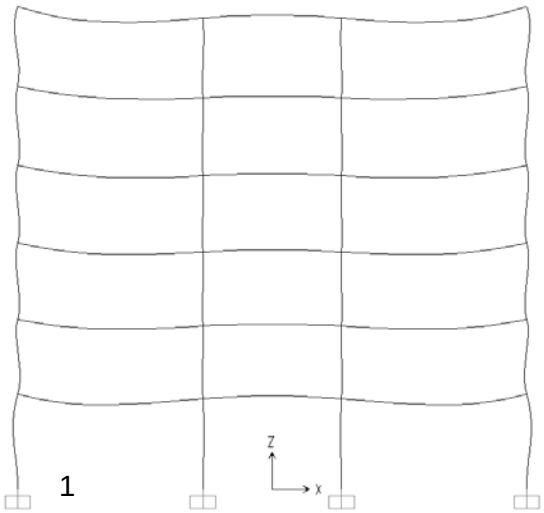

1

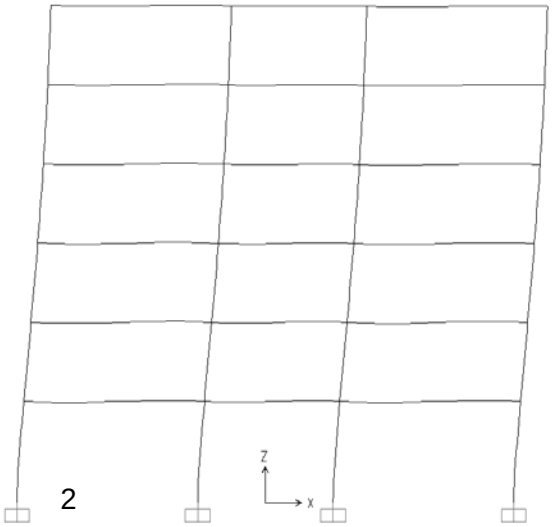

2

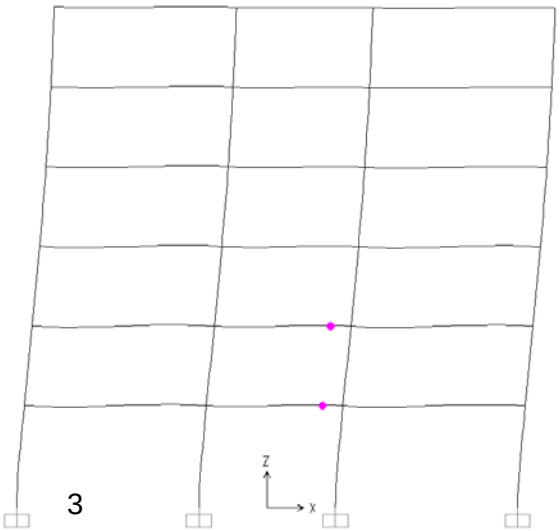

3

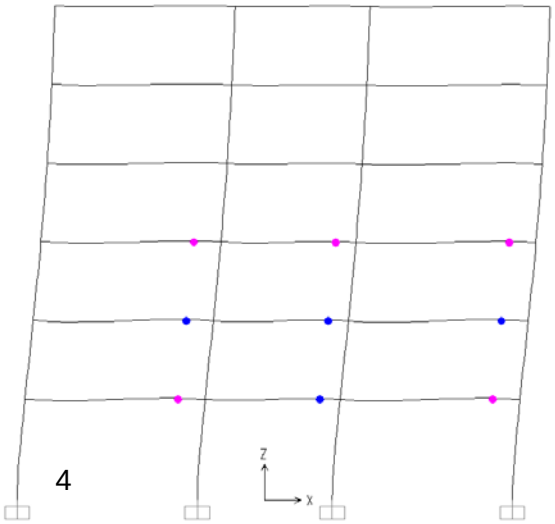

4

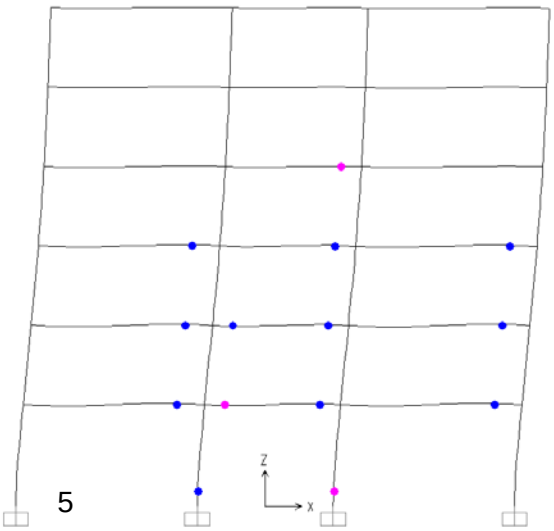

5

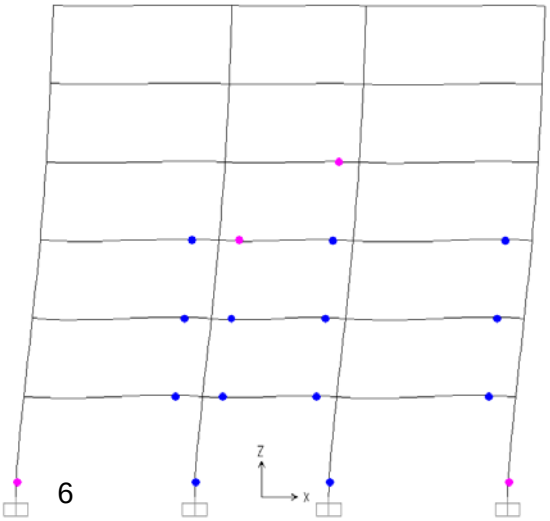

6

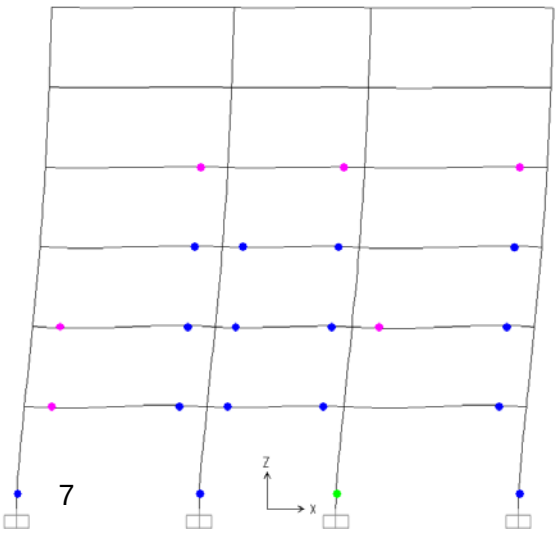

7

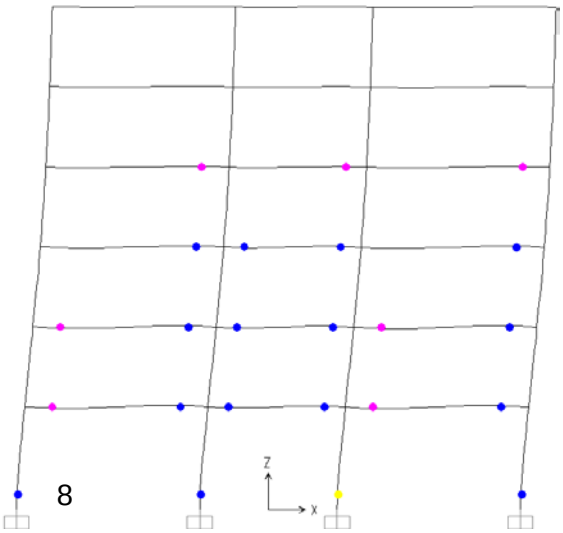

8

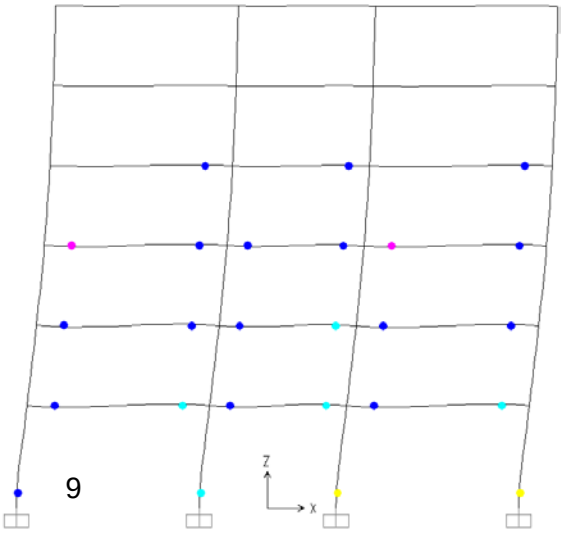

9

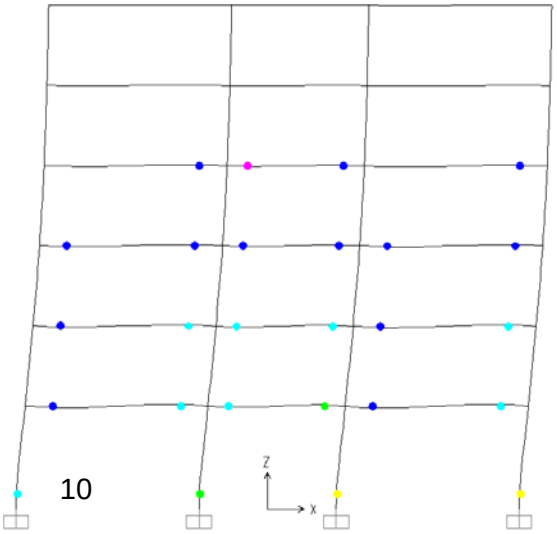

10

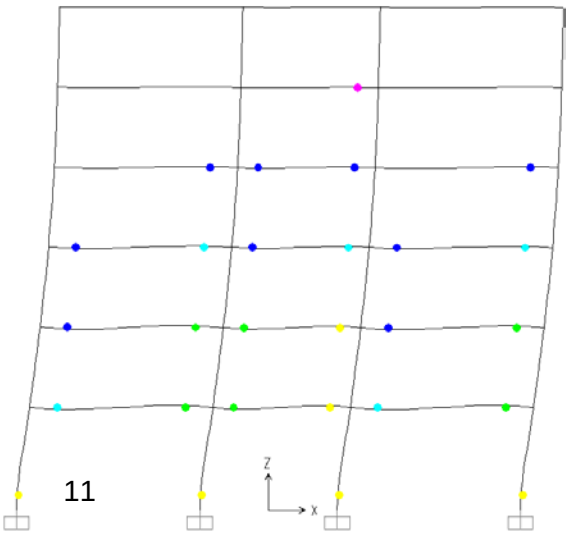

11

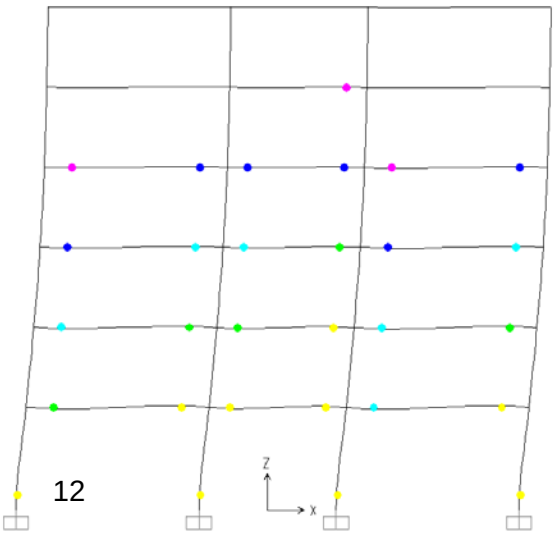

12

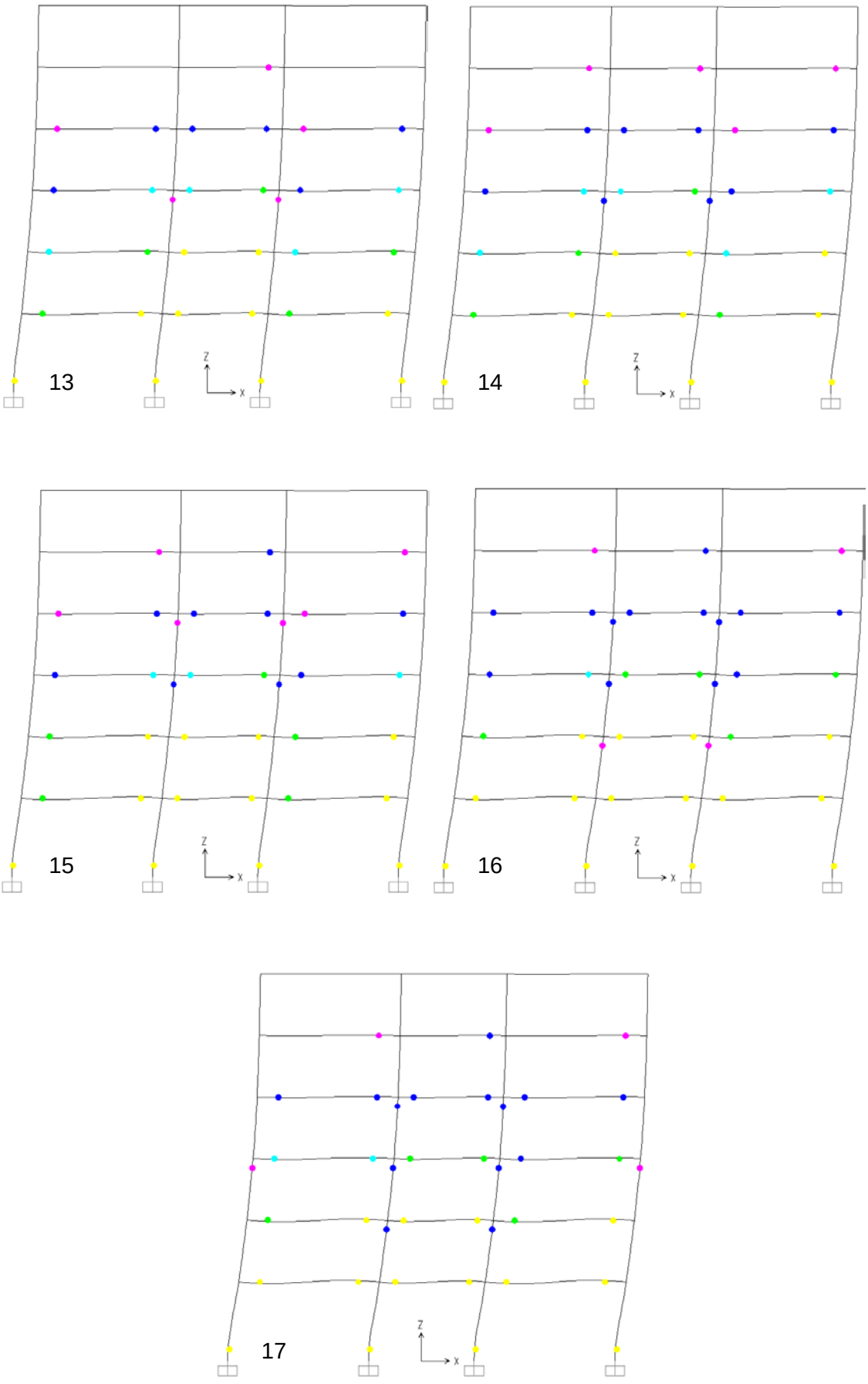

Figure 4.4. Hinge formation evolution of RMRF-S-S

As it can be observed in Figure 4.4, the first hinges appear in the second and third storeys in the beams. As the horizontal force increases more hinges appear in the beams until is reached a point where four hinges appear in the base of the columns. The horizontal force keeps increasing and the hinges keep dissipating energy by reaching a more critical state and appearing in the upper storeys. Then, more hinges appear in the internal columns. In the failure state, there are hinges in the external columns.

The frame in Figure 4.4 has all its members of stainless steel. For the other cases, the hinges do not reach the fifth storey, only get the forth. This fact, shows the great ability of dissipating energy of the stainless steel.

This behavior is the expected because this frame has been designed following the “strong-columns-weak-beams” rule. So, hinges tend to appear mostly in the beams.

The capacity curves obtained from the pushover analysis for the different RMRFs are shown in Figure 4.5.

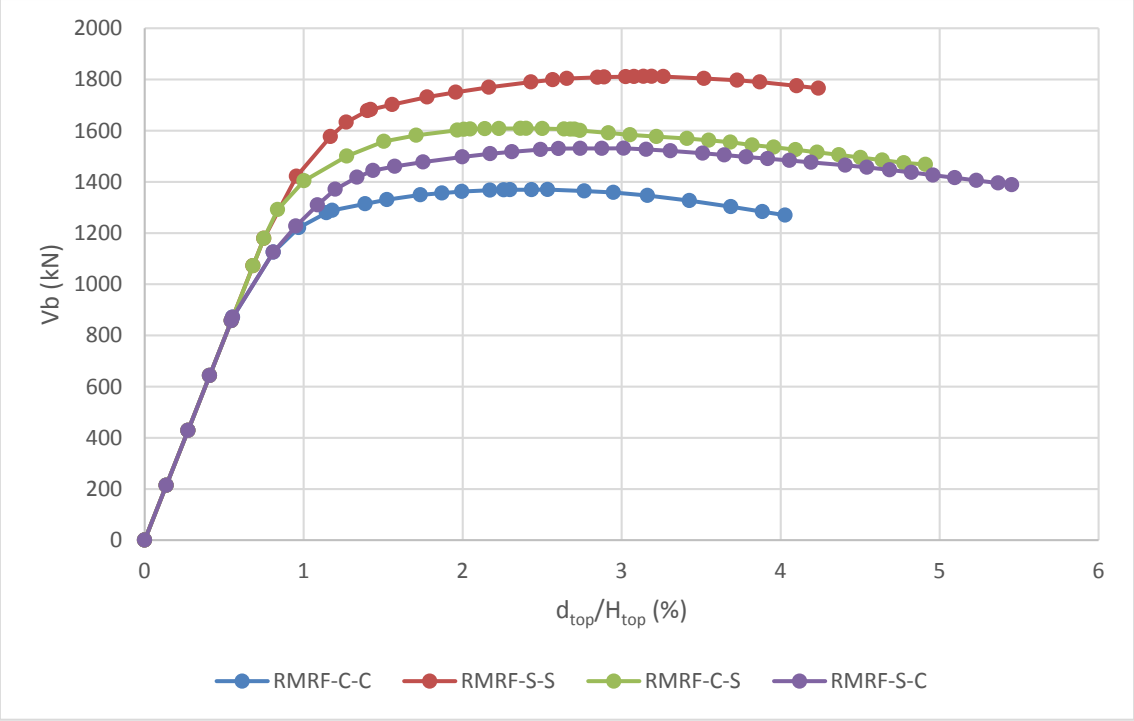

Figure 4.5. RMRF capacity curves

As it was expected, the frame with all its members of carbon steel is the curve with the lowest values of shear basal force and the frame with all its members of stainless steel is the curve with the highest values of basal shear force. In the following section, these results are going to be explained and analyzed in detail.

The values of the shear basal force (V) and displacement of the top of the frame (d) for yielding (y) and failure (u) are shown in Table 4.3. It is reminded that V_y and d_y are the shear basal force and the top displacement respectively when the first hinge appears and V_u and d_u are the shear basal force and top displacement at failure.

	V_y (kN)	V_u (kN)	d_y (m)	d_u (m)
RMRF-C-C	858	1370	0,12	0,56
RMRF-S-S	858	1811	0,12	0,69
RMRF-C-S	858	1606	0,12	0,59
RMRF-S-C	858	1531	0,12	0,66

Table 4.3. Yielding and ultimate values of capacity curves of RMRFs

In this case, the first hinge appears for the same shear basal force and with the same top displacement for all the RMRFs. This fact is logical because both materials have been defined with the same yielding stress and Young's modulus.

4.2.2. CBF

In this section, the hinge formation evolution, the capacity curves of CBFs and their main values of the capacity curves are presented in this order. In Figure 4.6 the hinge formation evolution of CBF is shown.

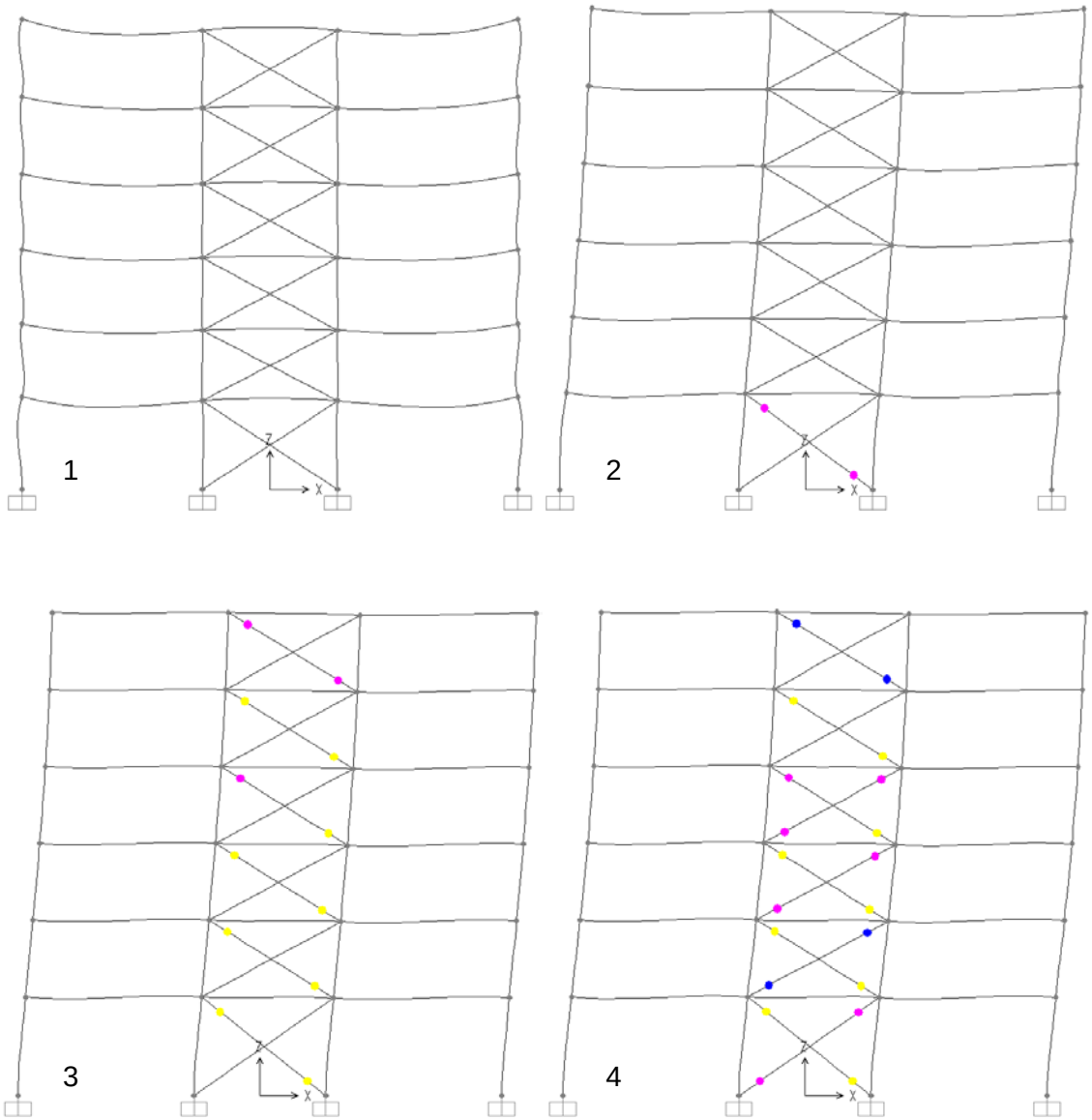

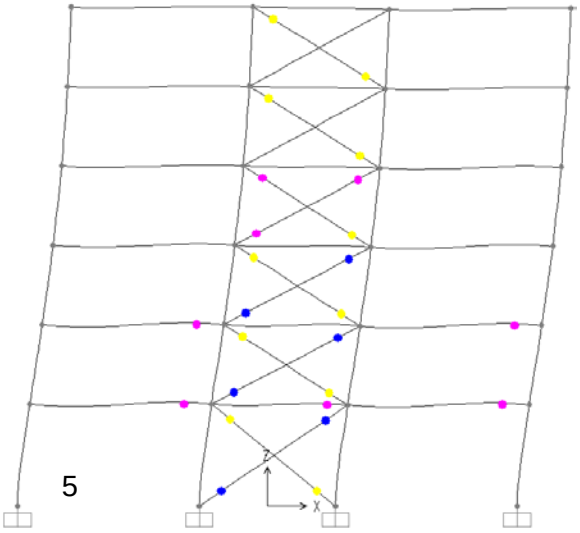
5

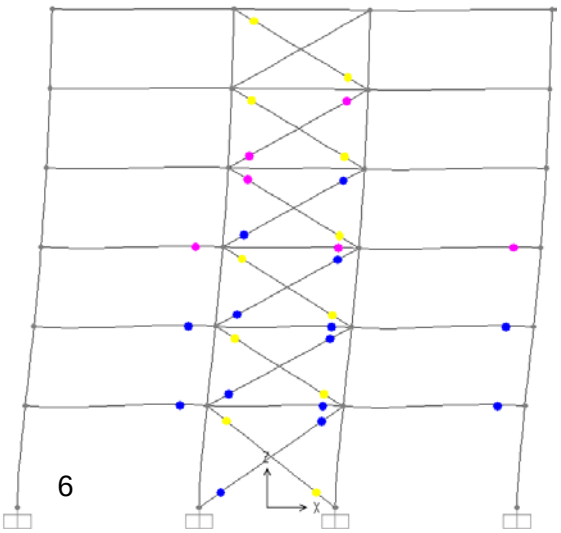
6

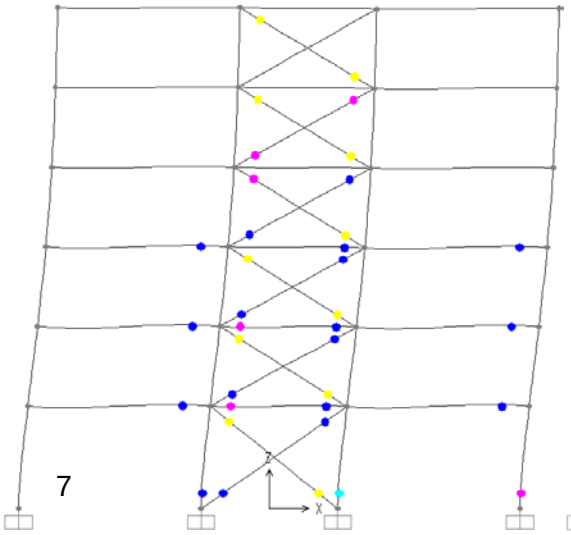
7

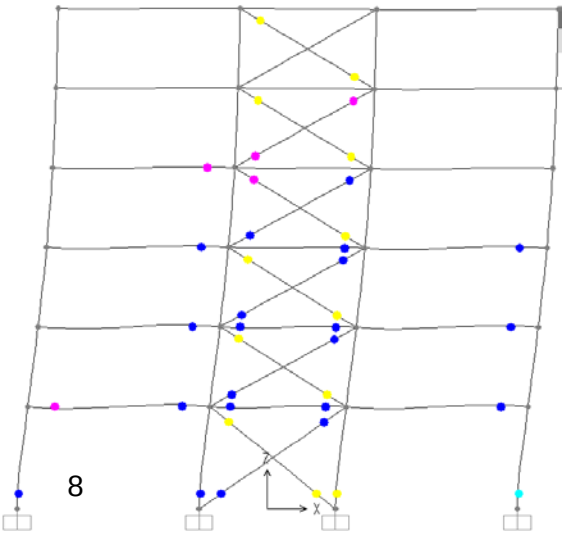
8

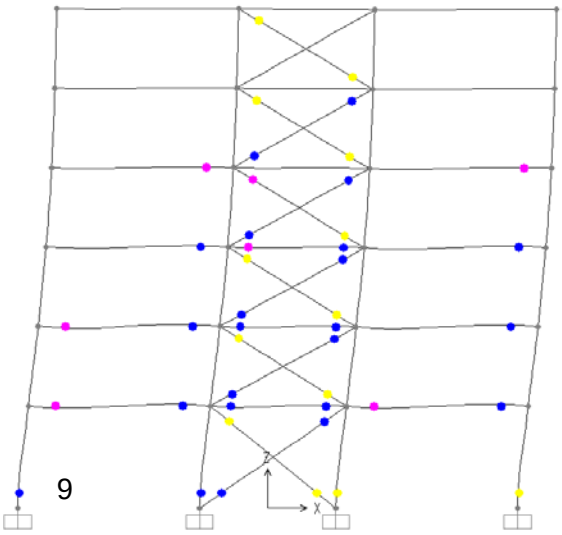
9

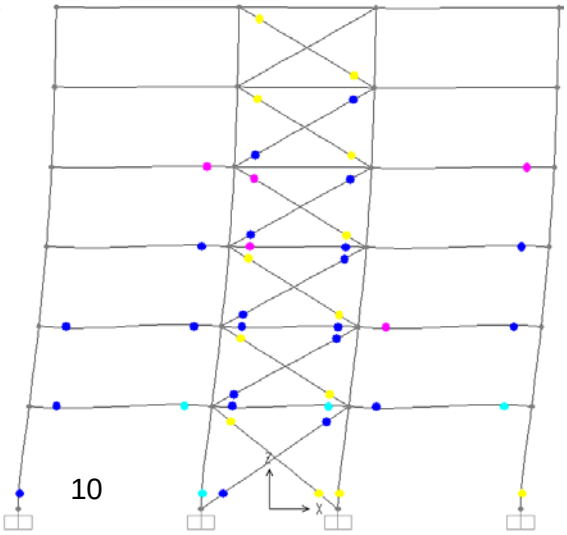
10

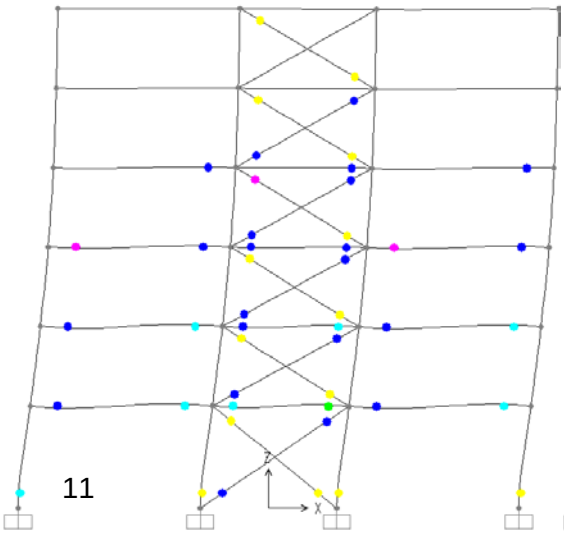
11

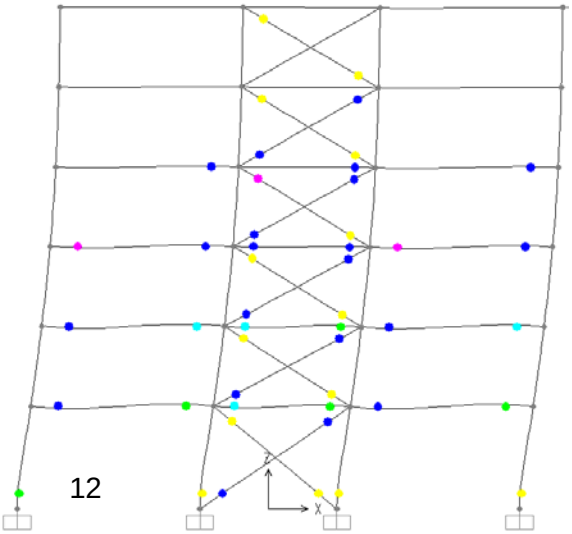
12

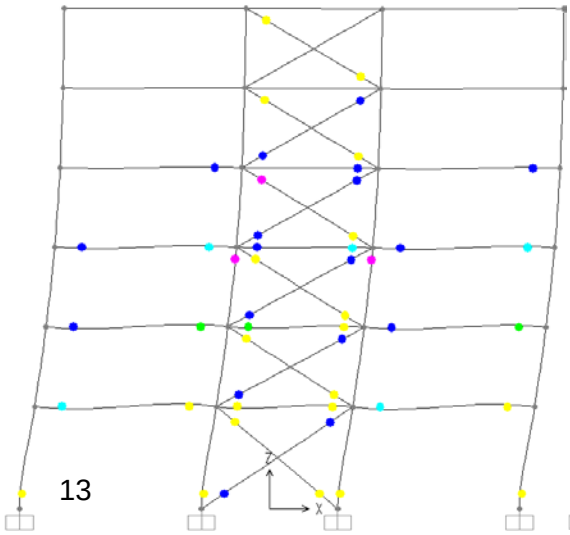
13

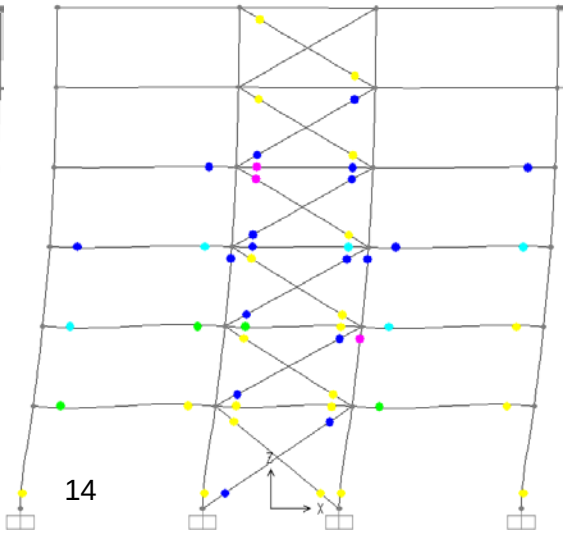
14

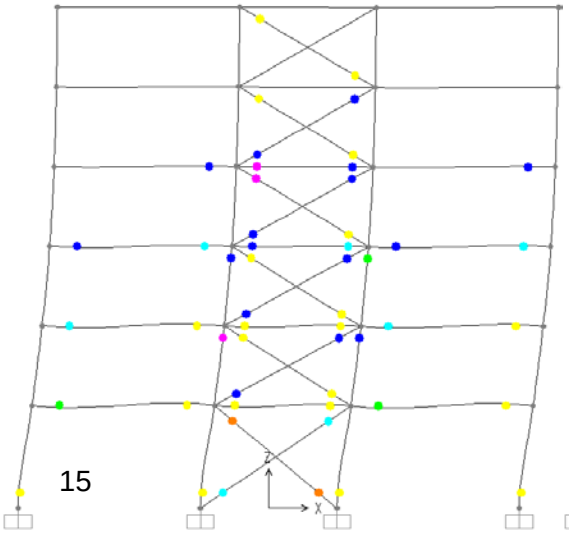
15

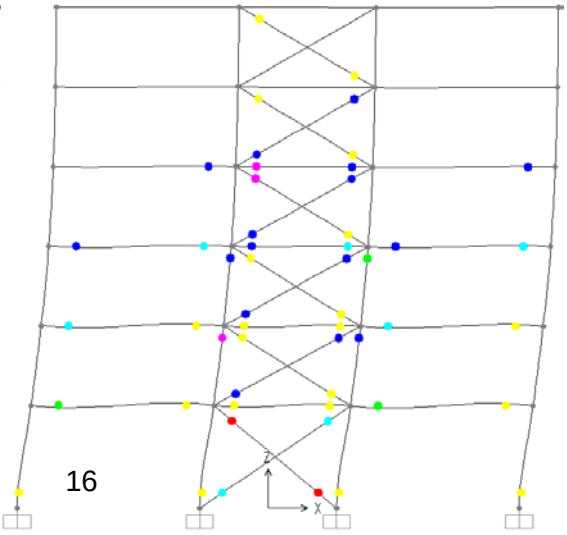
16

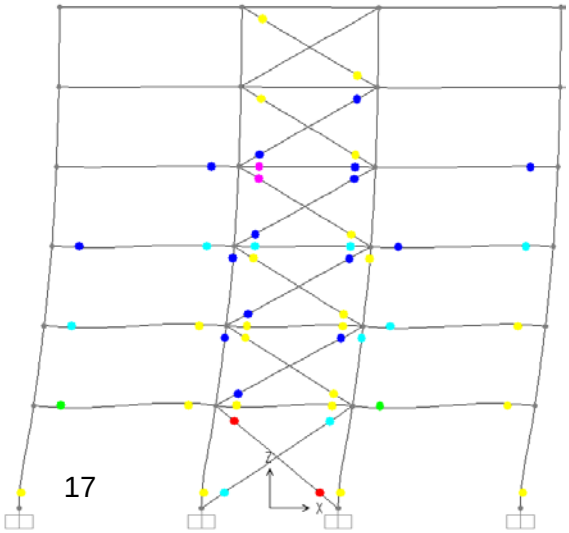

Figure 4.6. Hinge formation evolution of CBF-C-C-C

As it can be observed in Figure 4.6, the first hinges appear in the braces of the floor, and they quickly spread to the braces of the whole frame. Then, hinges start to appear in the beams of the first and second storey and coming up to the third and fourth. After that, the hinges in the base of the columns appear while the others already formed reach more critical states of deformation and dissipation of energy. Then, hinges in the internal columns appear along their longitude and the failure it is reached when the braces of the base collapse.

The hinge formation in Figure 4.6 follows the same patron of the other combinations of materials, but as the stainless steel content increases more hinges are formed in the upper storeys in the beams.

The capacity curves obtained from the pushover analysis of all the CBFs are shown in Figure 4.7.

As it was expected, the frame with all its members of carbon steel is the curve with the lowest values of shear basal force and the frame with all its members of stainless steel is the curve with the highest values of basal shear force. A similar behavior has been observed for RMRF cases, as highlighted before. In the following section, these results are going to be explained and analyzed in detail.

The values of the shear basal force (V) and displacement of the top of the frame (d) for yielding (y) and failure (u) are shown in Table 4.4. It is reminded that V_y and d_y are the shear basal force and the top displacement respectively when the first hinge appears and V_u and d_u are the shear basal force and top displacement at failure.

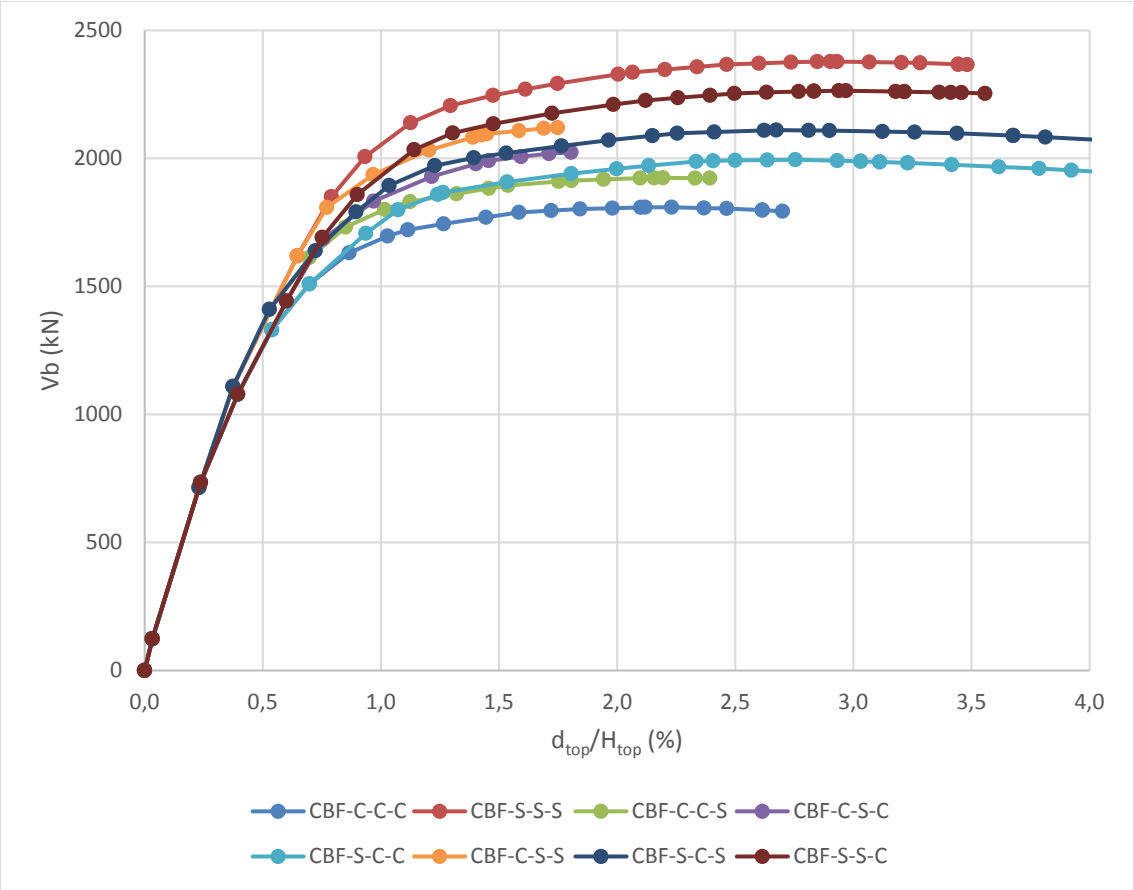

Figure 4.7. RMRF capacity curves

	V_y (kN)	V_u (kN)	d_y (m)	d_u (m)
CBF-C-C-C	1079	1809	0,087	0,466
CBF-S-S-S	714	2378	0,051	0,639
CBF-C-C-S	1109	1924	0,082	0,482
CBF-C-S-C	734	2024	0,052	0,397
CBF-S-C-C	734	1989	0,052	0,685
CBF-C-S-S	1109	2120	0,082	0,385
CBF-S-C-S	1109	2110	0,082	0,588
CBF-S-S-C	734	2264	0,052	0,653

Table 4.4. Yielding and ultimate values of capacity curves of CBFs

For CBFs, the first hinge does not appear for the same shear basal force and top displacement. This fact is because of the braces, whose presence implies a very different structural behavior. So, the use of a different material changes much more the global response of the frame.

4.3. Analysis of the results

In this section the results presented in the previous section are analyzed and evaluated. A comparison between RMRFs and CBFs behavior has been made and RMRFs and CBFs capacity curves have been studied and analyzed by fixing some parameters and changing the others. The system's overstrength and the ductility of each frame have been calculated as well. Furthermore, a simple and preliminar economic analysis has been carried out. It has been calculated the additional cost of using stainless steel for every case and related with the overstrength increase that this stainless steel causes to the frame. Finally, all these values obtained from the pushover analysis are compared with the values given by the EN-1998 in order to see if the standard gives conservative values or not.

In Figure 4.8 the capacity curves of the RMRF and CBF are shown. It only has been considered necessary to show the cases where the whole frames are made with carbon steel or stainless steel. The other cases would make more difficult the comparison between these structural typologies.

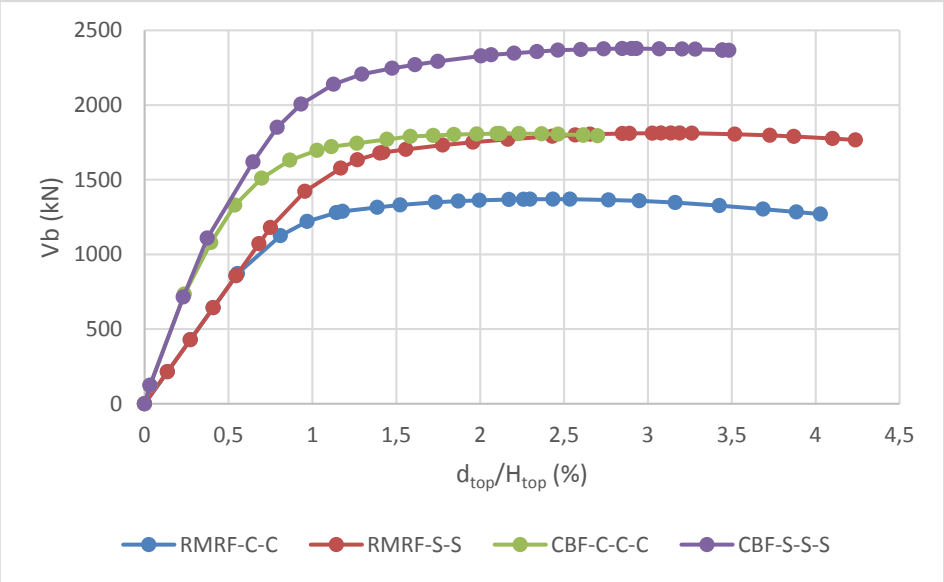

Figure 4.8. RMRFs and CBFs capacity curves

From Figure 4.8 can be observed that CBFs are more rigid than RMRFs, it can be easily deducted because the CBFs have higher slopes than RMRFs capacity curves in the elastic part of the curve. This, as it has already highlighted, is due to the presence of the braces, whose function is to reduce the deformability of the frames.

The overstrenght (q) and ductility (μ) values of these frames are shown in Table 4.5. Overstrenght has been computed dividing V_u by V_y ($q= V_u/ V_y$) and the ductility dividing d_u by d_y ($\mu= d_u/ d_y$). V_u, V_y, d_u and d_y values are shown as well.

	V_y (kN)	V_u (kN)	d_y (m)	d_u (m)	q	μ
RMRF-C-C	858	1370	0,120	0,558	1,60	4,65
RMRF-S-S	858	1812	0,120	0,690	2,11	5,75
CBF-C-C-C	1079	1809	0,0867	0,466	1,68	5,38
CBF-S-S-S	714	2378	0,0506	0,639	3,33	12,61

Table 4.5. Overstrength and ductility values of RMRFs and CBFs

Regarding the overstrength, it can be observed that for the RMRF and CBF carbon steel frames the q value is very similar. And this value is very similar to the f_u/f_y=1,59 of the material too, which it has many sense. Stainless steel frames, as a rule, present higher values of overstrength. The most ductile frame of the Table 4.5 is the CBF-S-S-S and as it was expected, stainless steel frames are more ductile than the carbon steel ones. It could be said that the frames behave like the material of their elements.

After comparing the RMRF and CBF behavior trough capacity curves, overstrength and ductility values of the different RMRFs will be analyzed in detail. Hence, for this purpose in Figure 4.9 capacity curves of RMRF are shown again.

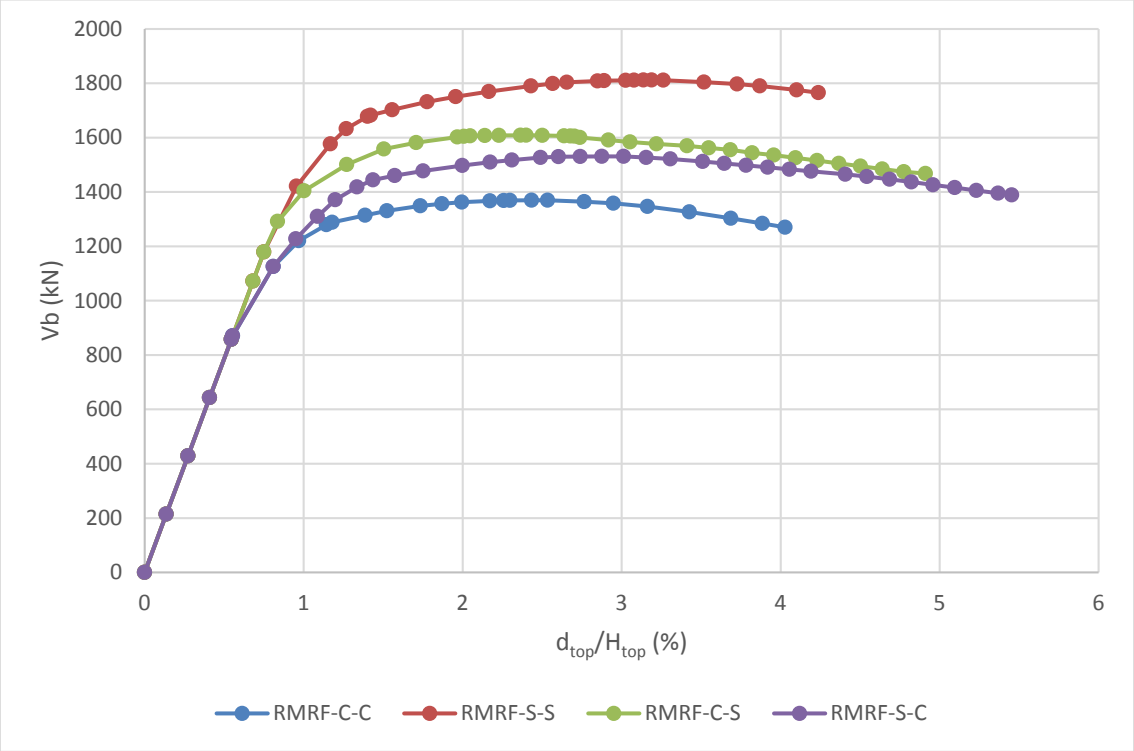

Figure 4.9. RMRF capacity curves

It has already mentioned that stainless steel frames show the highest values of ultimate shear basal force while carbon steel frames show the lowest values. But between these curves two other curves have been computed: one of them corresponds to the frame with its beams made from stainless steel and its columns from carbon steel and the other one corresponds to the frame with carbon steel beams and stainless steel columns. These curves are shown in Figure 4.9 in grey and in yellow respectively.

The overstrenght and ductility values of these frames are shown in Table 4.6. V_u, V_y, d_u and d_y values are shown as well.

	V_y (kN)	V_u (kN)	d_y (m)	d_u (m)	q	μ
RMRF-C-C	858	1370	0,120	0,558	1,60	4,65
RMRF-S-S	858	1812	0,120	0,690	2,11	5,75
RMRF-C-S	858	1606	0,120	0,589	1,87	4,91
RMRF-S-C	858	1531	0,120	0,663	1,79	5,52

Table 4.6. Overstrength and ductility values of RMRFs

From Table 4.6 can be observed that for the four different RMRFs, the first hinge is formed at the same ultimate shear basal force and the same displacement of the top of the frame. This fact is logical due to both materials, stainless steel and carbon steel have been defined with the same yield stress and Young's modulus.

RMRF-C-S shows higher values of ultimate shear basal force than RMRF-S-C, which is logical because, mostly, the hinges are formed in the beams, which are supposed to be of stainless steel. So, if the material has a higher ultimate strength, the frame will be more resistant (higher V_u value). The overstrength value shows the same effect: is greater for the RMRF-C-S than for RMRF-S-C.

Regarding the ductility, RMRF-S-C presents a higher μ value than the RMRF-C-S. This fact could be explained because a hinge in a column entails a higher displacement in the top of the frame than a hinge in a beam. If a hinge in a column is able to allow more rotation (because is made with stainless steel) it is logical that this fact implies more global deformation of the frame.

The CBFs are going to be analyzed by fixing one element of carbon steel and changing the other members of material in order to see clearly the benefits of using stainless steel to improve the seismic performance of a framed structure.

So, the cases with the columns of carbon steel are presented and analyzed. In order to comment the results properly in Figure 4.10 capacity curves of CBF-C-C-C, CBF-C-C-S, CBF-C-S-C and CBF-C-S-S are shown.

From Figure 4.10 is deducted that if the braces are made with stainless steel the ultimate strength of the frame does not vary too much. If only the beams are changed to stainless steel the ultimate strength undergo a slightly increase compared to CBF-C-C-S. As it was expected, the maximum ultimate strength of these cases shown in Figure 4.10 is found for the frame with stainless steel braces and stainless steel beams. In Table 4.7 overstrength (q) and ductility (μ) values are shown.

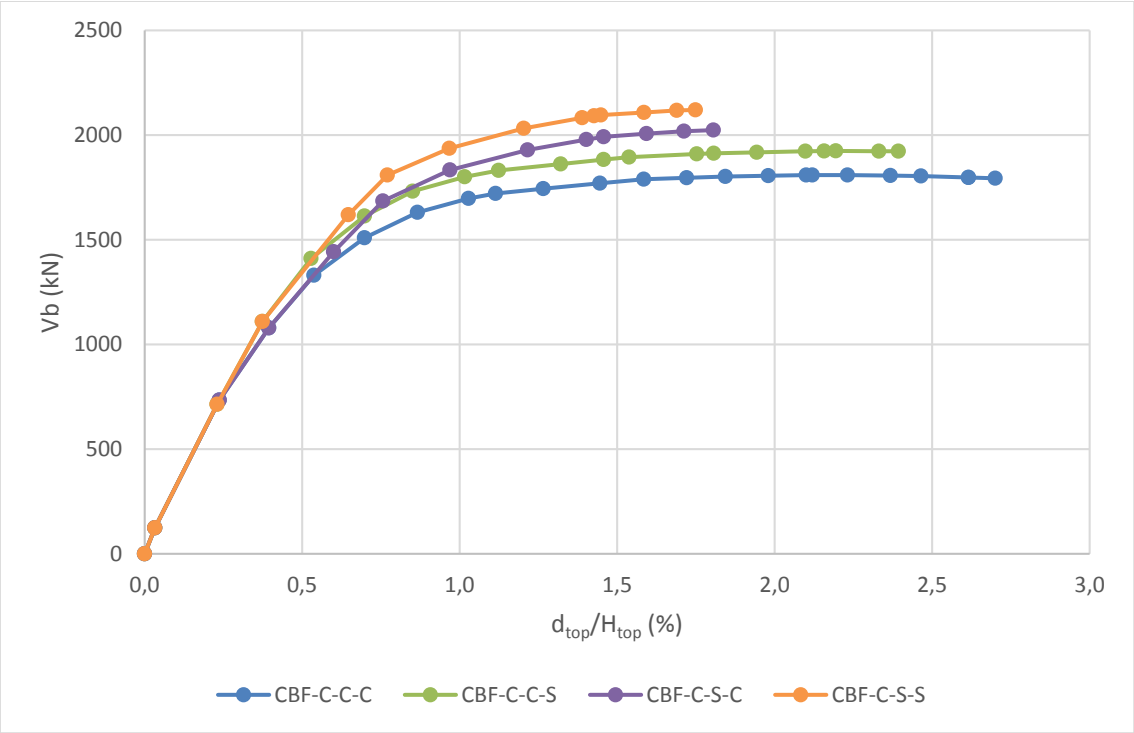

Figure 4.10. Capacity curves of the CBFs with carbon steel columns

	V_y (kN)	V_u (kN)	d_y (m)	d_u (m)	q	μ
CBF-C-C-C	1079	1809	0,0867	0,466	1,68	5,38
CBF-C-C-S	1109	1924	0,0823	0,483	1,73	5,86
CBF-C-S-C	734	2024	0,0522	0,397	2,76	7,62
CBF-C-S-S	1109	2120	0,0823	0,385	2,97	4,67

Table 4.7. Overstrength and ductility values of CBFs with carbon steel columns

The overstrength of the system presents increasing values as the stainless steel content in the frame increases. If stainless steel is used only in braces the overstrength slightly increases but, if stainless steel is used in the beams or in the beams and braces, the overstrength reaches higher values. On the other hand, the ductility increases too as the stainless steel content of the frame heighten but not for CBF-C-S-S. This fact could be explained by a little difference in the hinge formation that makes the structure collapse earlier or by an error of the software that stop the calculations in a too early step.

In this occasion the frames with carbon steel beams are going to be analyzed in detail. So, the capacity curves of the CBFs with their beams made of carbon steel are shown in Figure 4.11.

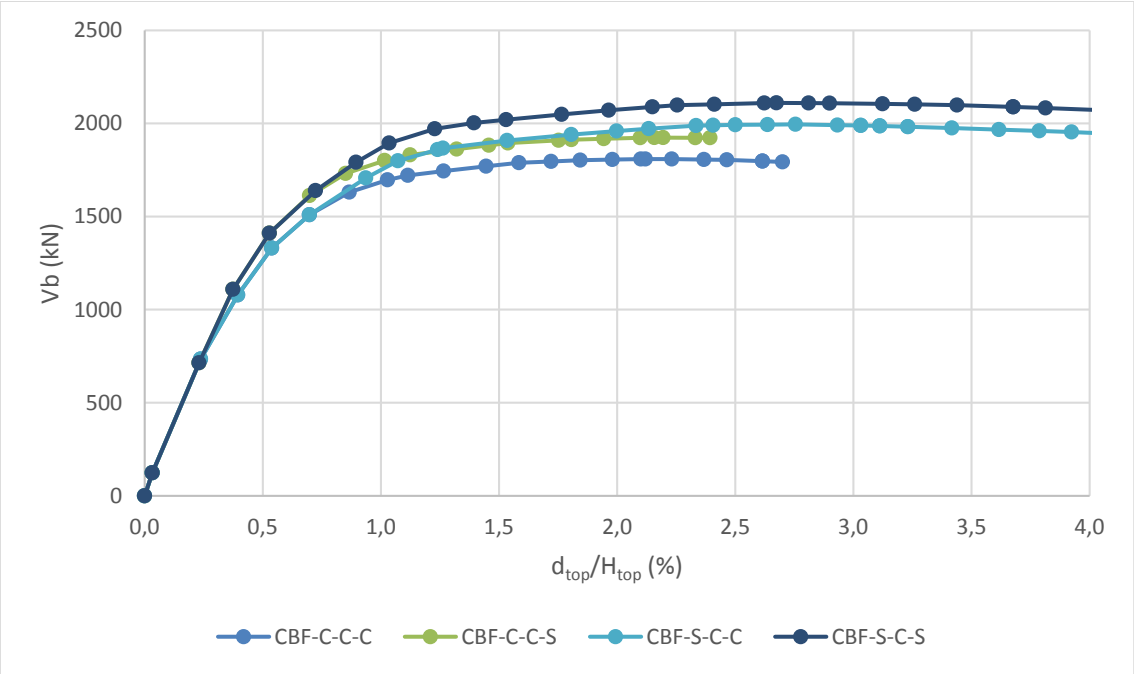

Figure 4.11. Capacity curves of the CBFs with carbon steel beams

Here, from Figure 4.11 it can be observed that in terms of ultimate capacities, the difference between using stainless steel in braces or in columns it is not important, but it is, in fact, in terms of ductility. As it has been deducted in the previous case, as the stainless steel content increases the ultimate shear basal force increases too. That is why in Figure 4.11 the CBF-S-C-S presents the highest values of ultimate strength. In Table 4.8 the overstrength and ductility values of the CBFs with carbon steel beams are shown.

	V_y (kN)	V_u (kN)	d_y (m)	d_u (m)	q	μ
CBF-C-C-C	1079	1809	0,0867	0,466	1,68	5,38
CBF-C-C-S	1109	1924	0,0823	0,483	1,73	5,86
CBF-S-C-C	734	1989	0,0521	0,685	2,71	13,13
CBF-S-C-S	714	2110	0,0506	0,588	2,95	11,62

Table 4.8. Overstrength and ductility values of CBFs with carbon Steel beams

Again, it is observed that the highest values of overstrength are found for the case of two members made of stainless steel. It is noted a big gap of overstrength value between the benchmark or the case with only stainless steel braces and the cases with the stainless steel columns or stainless steel columns and braces. It happens the same with the ductility, when the stainless steel content is elevated, q and μ are elevated too.

Now, carbon steel is going to be fixed in the braces: so, the capacity curves of the CBFs with their braces of carbon steel are shown in Figure 4.12.

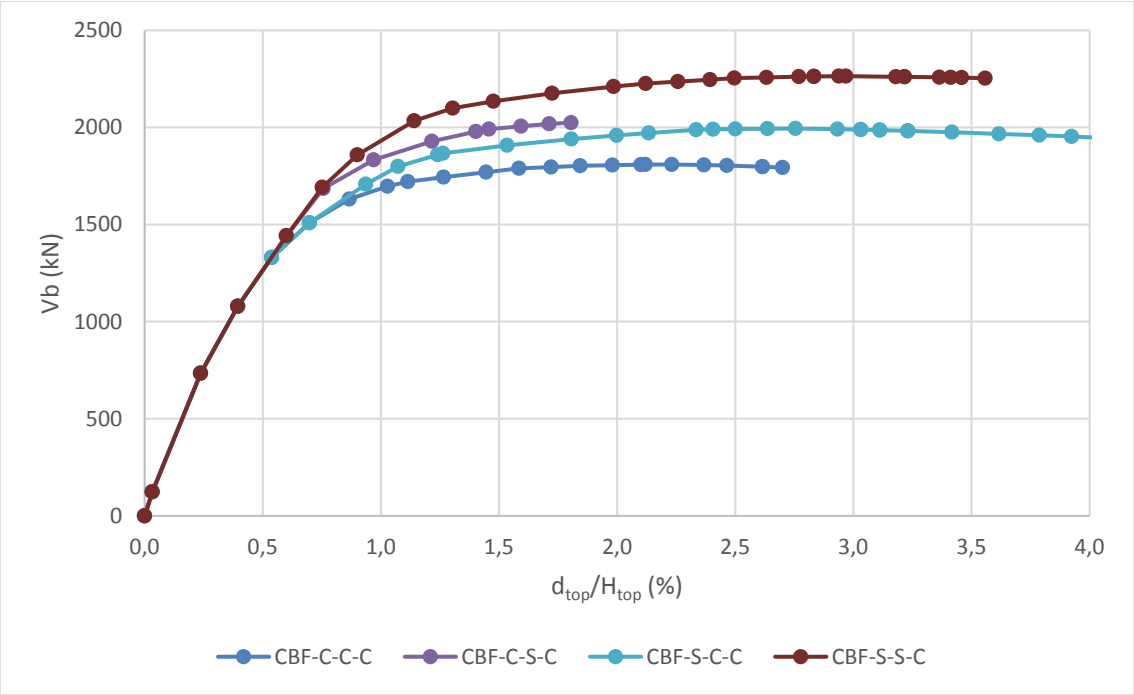

Figure 4.12. Capacity curves of the CBFs with carbon steel braces

In this case, from Figure 4.12 can be deducted that the frame with stainless steel columns and beams shows by far the highest ultimate capacity, followed by the one with only the beams of stainless steel, then by the one with only stainless steel columns and finally the benchmark. It is a logical order because the hinges are formed mainly in the beams, so, the ultimate capacity when the beams are made of stainless steel is greater than when this does not happen.

To interpret the results shown in Figure 4.12, the overstrength and ductility values of the CBFs with carbon steel braces are shown in Table 4.9.

	V_y (kN)	V_u (kN)	d_y (m)	d_u (m)	q	μ
CBF-C-C-C	1079	1809	0,0867	0,466	1,68	5,38
CBF-C-S-C	734	2024	0,0522	0,397	2,76	7,62
CBF-S-C-C	734	1989	0,0522	0,685	2,71	13,13
CBF-S-S-C	734	2264	0,0522	0,653	3,08	12,52

Table 4.9. Overstrength and ductility values of CBFs with carbon steel braces

As it can be noted from Table 4.9 the results show a similar behavior from the cases studied before. There is an important gap between the overstrength and ductility values of frames without stainless steel and frames with it. And the highest value of overstrength is found in the frame with beams and columns of stainless steel.

As it has been said, as the stainless steel content heighten, q and μ increase. To see this behavior better it has been computed the weight of each component of the frame, in order to calculate the stainless steel content of every case of study. These weigh calculations has been made for both kinds of frames: RMRFs and CBFs. In Table 4.10 and Table 4.11 RMRFs and CBFs weighs are shown respectively.

	Length (m)	Kg/L	Weight (Kg)
IPE500	110	90,7	9977
IPE400	22	66,3	1458,6
HEB500	44	187,3	8241,2
HEB400	44	155,3	6833,2
Total	220		**26510**

Table 4.10. Weighs of the elements of RMRF

	Length (m)	Kg/L	Weight (Kg)
IPE500	110	90,7	9977
IPE400	22	66,3	1458,6
HEB500	44	187,3	8241,2
HEB400	44	155,3	6833,2
H115	84,46	0,006	0,48
Total	304,46		26510,48

Table 4.11. Weighs of the elements of CBF

With the data showed in Table 4.10 and Table 4.11 it is possible to calculate the stainless steel content of every frame of study. So, in Table 4.12 for RMRF and in Table 4.13 for CBF overstrenght and ductility values, related with stainless steel content are shown.

It is reminded that the first capital letters of the nomenclature of the cases show the frame type. After the first hyphen there is a capital letter related with the material of the columns, after the second hyphen there is the letter of the beams material and after the third hyphen there is the letter of the braces material. C and S mean carbon steel and stainless steel respectively.

	q	μ	% SS
RMRF-C-C	1,60	4,65	0
RMRF-C-S	1,87	4,91	43,14
RMRF-S-C	1,79	5,52	56,86
RMRF-S-S	2,11	5,75	100

Table 4.12. Overestrength and ductility values with the stainless steel content for RMRFs

	q	μ	% SS
CBF-C-C-C	1,68	5,38	0
CBF-C-C-S	1,73	5,86	0,002
CBF-C-S-C	2,76	7,62	43,14
CBF-C-S-S	2,97	4,67	43,14
CBF-S-C-C	2,71	13,13	56,86
CBF-S-C-S	2,95	11,62	56,86
CBF-S-S-C	3,08	12,52	99,998
CBF-S-S-S	3,33	12,61	100

Table 4.13. Overestrength and ductility values with the stainless steel content for CBFs

In general terms, as it has already noted, as the stainless steel content increases the overstrength and ductility rises too. In order to characterize this behavior, in Figure 4.13 and Figure 4.14 the numbers of the overstrength in Table 4.12 and Table 4.13 are plotted for RMRFs and CBFs respectively.

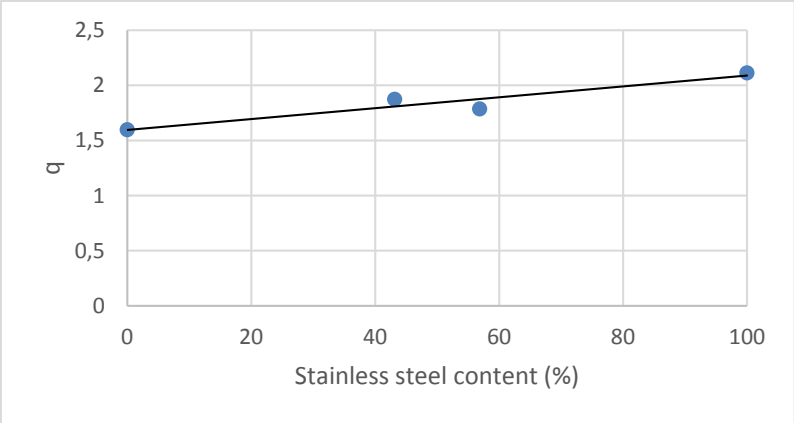

Figure 4.13. Overstrength against stainless Steel content in RMRFs

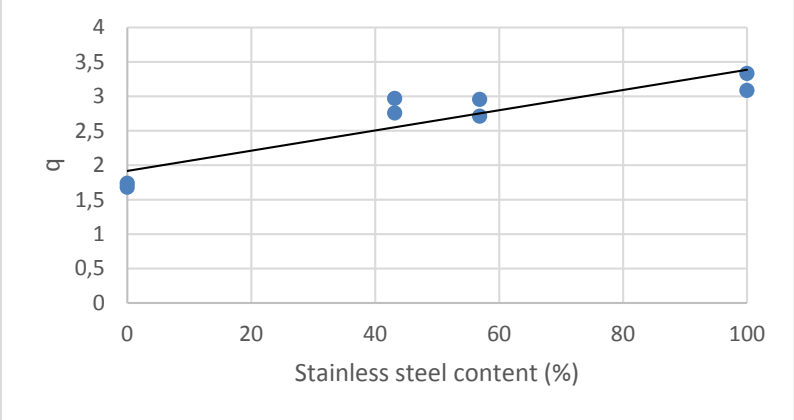

Figure 4.14. Overstrength against stainless Steel content in CBFs

In Figure 4.15 and Figure 4.16 are shown the same graphics but for the ductility value.

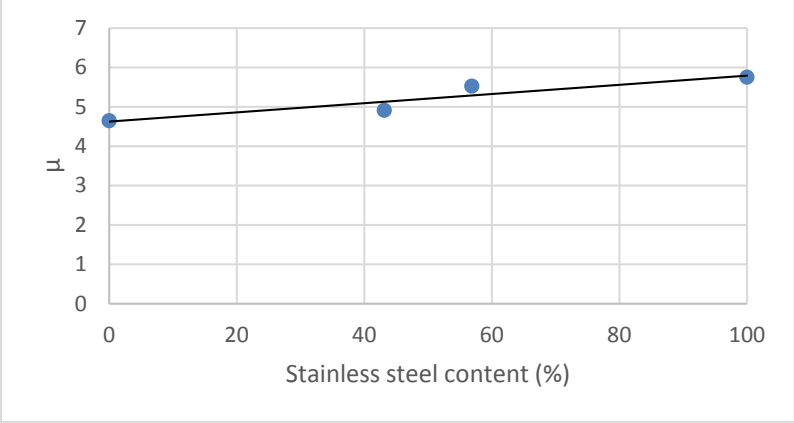

Figure 4.15. Ductility against stainless steel content in RMRFs

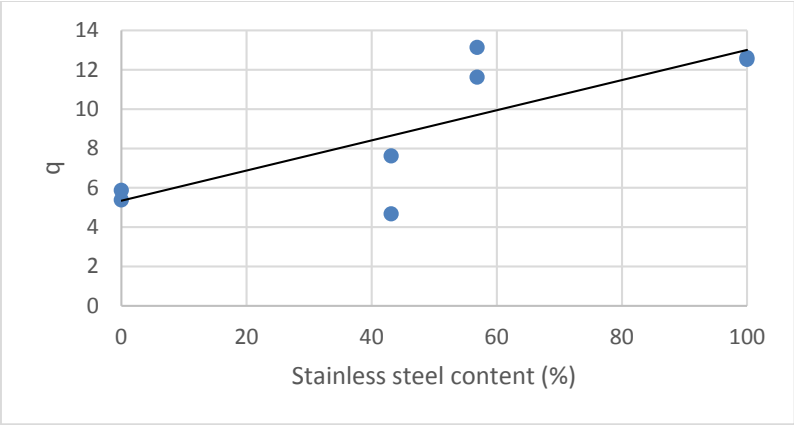

Figure 4.16. Ductility against stainless steel content in CBFs

As it has already been mentioned, and the lineal regression shows it, the overstrenght and ductility rise when the stainless steel content increases. Depending on the case, the line is closer to the points. It can be highlighted that the frames behave like this but it would be necessary to run more analysis to obtain more points and verify with more arguments this behavior.

In the following analysis the extra cost of using stainless steel will be compared with the structural benefits obtained from this additional cost. It has been assumed that austenitic stainless steel is four times more expensive than carbon steel.

In Table 4.14 and Table 4.15 the additional cost of using stainless steel and the increment of overstrength are shown for RMRFs and CBF respectively.

	Additional cost (%)	Δq (%)
RMRF-C-C	0	0
RMRF-C-S	129,4	17,3
RMRF-S-C	170,6	11,8
RMRF-S-S	300	32,3

Table 4.14. Additional cost and overstrength increment for RMRFs

	Additional cost (%)	Δq (%)
CBF-C-C-C	0	0
CBF-C-C-S	0,005	3,5
CBF-C-S-C	129,4	64,4
CBF-C-S-S	129,4	77,0
CBF-S-C-C	170,6	61,6
CBF-S-C-S	170,6	76,2
CBF-S-S-C	299,9	83,9
CBF-S-S-S	300	98,5

Table 4.15. Additional cost and overstrength increment for CBFs

From these two tables (Table 4.14 and Table 4.15) can be noted that the only case where the additional cost is lower than the overstrength increment is the CBF-C-C-S. In

this case with an additional cost is 0,005% while the increment of overstrength is 3,5%. Although it may be considered a good result, the increment of the overstrength is very low.

For further studies it should be considered the possibility of only use the stainless steel at the end of some elements and connections. Most probably, acting like this, it could be achieved higher overstrength values with a lower stainless steel content. Cheaper frames with higher overstrength values. But in this case, it should be taken into account the additional cost of the need of placing more connections.

This preliminar economic study only has taken into account the direct costs of the material. But it has been commented in the state of art of this study, stainless steel presents many advantages respect carbon steel such as maintenance costs, almost non-existent.

Furthermore, stainless steel has a better behavior against fire. This property is very important if related with the seismic action. When an earthquake takes place, fire is likely to appear too. This fact allows to design the same structure with smaller cross-sections, which reduce the global weigh, the dimensions of the foundations and consequently the direct building cost.

Stainless steel frames achieve higher values of overstrength (q). This fact allows to reduce the response spectrum and consequently design the structure with smaller cross-section types with the corresponding economic benefits already commented.

Stainless steel use gives to the structure high ductility values. This fact may avoid the possible need of place an isolated base system which would suppose an important additional cost.

4.4. EN-1998 assessment

The shear basal force of design has been computed by meanings of EN-1998. The shear basal force of design (V_d), the ultimate shear basal force (V_u) and the V_u/V_d ratio are shown in Table 4.16 and in Table 4.17 for all the frames of study, RMRFs and CBFs respectively.

The basal shear basal force of design of RMRFs is approximately the half of CBFs because the fundamental period of the CBFs computed by the EN-1998 simplified formula is very close to the period of the seism of design and the type ground of study (ground type B). Hence, the resonance phenomena takes place. This fact does not appears in RMRF. For this reason, the CBFs V_u/V_d ratios are lower for CBFs.

EN-1998 establishes an upper limit of overstrength value (q) for RMRFs and CBFs and is equal to 4 for medium ductility class structures. For the cases of this study, the EN-1998 gives a fairly value of q for RMRF. For CBFs, the standard allows to choose a too optimistic value of q to compute the shear basal force of design. It is true that this analysis is closely related with the fundamental period of the structure, in order to conclude a confident verdict of the reliance of the EN-1998 for CBFs, different CBFs should be analyzed.

	V_y (kN)	V_d (kN)	V_u (kN)	V_u/V_d
RMRF-C-C	858	441	1370	3,11
RMRF-S-S	858	441	1812	4,11
RMRF-C-S	858	441	1606	3,64
RMRF-S-C	858	441	1531	3,47

Table 4.16. RMRFs V_u/V_d ratios

	V_y (kN)	V_d (kN)	V_u (kN)	V_u/V_d
CBF-C-C-C	1079	900	1809	2,01
CBF-S-S-S	714	900	2378	2,64
CBF-C-C-S	1109	900	1924	2,14
CBF-C-S-C	734	900	2024	2,25
CBF-S-C-C	734	900	1989	2,21
CBF-C-S-S	714	900	2120	2,36
CBF-S-C-S	714	900	2110	2,34
CBF-S-S-C	734	900	2264	2,52

Table 4.17. CBFs V_u/V_d ratios

5. CONCLUSIONS AND OUTLOOK

12 modal and pushover analyses have been carried out in this study with the aim of evaluate the suitability of using stainless steel in seismic design. The seismic performance of RMRFs and CBFs has been studied. The different cases of study have been formed by changing the material of their elements (columns, beams and braces). The results are summarized herein.

The results obtained from the pushover analyses show the suitability of using stainless steel in seismic design. The frames modeled in stainless steel present higher values of overstrength and ultimate shear basal force, ductility values are higher as well. It has been seen that, as a rule, as the stainless steel content increases the ultimate shear basal force, overstrength and ductility value heighten.

Unfortunately, stainless steel is an expensive material, more or less four times the price of carbon steel. For the frames modeled in this study, the additional cost is always higher than the increment of overstrength excepting one case, the CBF with carbon steel beams and columns and stainless steel braces. The increment of overstrength in this case is only of 3,5 %.

It must be reminded that the economic study is very simple, it only has been taken into account the direct cost of the material. Connection costs and construction costs have not been computed. It must not be forgotten that stainless steel has almost non-existent maintenance costs, too. Furthermore, stainless steel has more advantages such as a better behavior against fire, which is very likely to appear when an earthquake takes place. This fact could suppose a saving in insulating paint or by designing the frame with smaller cross-sections. Probably, when stainless steel is used, due to greater values of q, the cross-sections could be smaller because q is the value used to reduce the response spectrums given by the standards. Another possible saving deducted from the obtained results could be that due to the stainless steel ductility, the construction of a seismic base isolator could be avoided. If all these factors had been considered, the economic analysis would have been more favorable to stainless steel.

It has been observed that better results arise from stainless steel beams frames. The frames have been designed under the “strong-column-weak-beam” rule, so, the hinges appear mostly in the beams. Hence, overstrenght values are higher when the frame has stainless steel beams. But in the other hand, when the frame has stainless steel columns and carbon steel beams the results show higher ductility than the frame with stainless steel beams and carbon steel columns. That is why the hinges in the columns entail higher top displacement, thus more ductility.

The overstrength values computed for the frames in this study has been compared with the q values proposed by EN-1998 and it has been concluded that the upper limit given by this standard gives is a reasonable one. But it must be cautious because some of the q values computed in this study are the half of the upper limit proposed by norm.

From the modal analyses, it has been concluded that the braces make the frames stiffener, thus braced frames has a lower fundamental periods.

From this study, it can be concluded that stainless steel has the adequate properties to obtain a good seismic performance. With an accurate design, a significant increment of ultimate resistance can be achieved with a low additional cost.

The cases computed in this study have been made with the whole members of one material. It has not been considered the possibility of making a part of a beam of stainless steel and the other part with carbon steel. For further studies, it would be interesting to make the ends of the elements of stainless steel and the other part of the elements of carbon steel. Whit this structural setup the plastic hinges would be formed in the stainless steel, allowing more deformation and reaching higher values of shear basal force. Furthermore, this frame, presumably, would achieve good ultimate shear basal force, and overstrength and ductility values with a low stainless steel content. Probably, in this frame the structural benefit would be higher than the additional cost in percent.

References

ArcelorMittal. Stainless Steel in construction: Building and Construction Support (BCS). 2nd Edition. Colchester.

Arrayago, I. (2011). Comportamiento estructural de vigas de acero inoxidable ferrítico frente a cargas concentradas. Universitat Politèctinca de Catalunya. 2011.

ASCE. (2000). American society of civil engineers. FEMA 356: Prestandard and commentary for the seismic rehabilitation of buildings. Washington DC: 2000.

ASCE. (2005). American society of civil engineers. FEMA 440: Improvement of nonlinear seismic analysis procedures. Washington DC: 2005.

ATC-40. (1996). Applied technology council. Seismic evaluation and retrofit of concrete buildings. Redwood City: 1996.

Barbat, AH and Bozzo, LM. (1999). Diseño sismorresistente de edificios: técnicas convencionales y avanzadas. 1st Edition. Barcelona: Raverté, 1999. ISBN 8429120114.

Barbat, AH and Oller, S. (2005). Cálculo y diseño sismorresistente de edificios: aplicación de la norma NCSE-02. 1st Edition. Barcelona: CIMNE, 2005. ISBN 8495999897.

Bozorgnia, Y and Campbell, KW. (2010). Analysis of Comulative Absolute Velocity (CAV) and JMA Instrumental Seismic Intensity using the PEER-NGA Strong motion Database. PEER Report, University of California, Pacific Earthquake Engineering Research Center. 2010.

Crisafulli, FJ. (2012). Diseño sismorresistente de estructuras de acero. Santiago: Asociación Latinoamericana del acero – Alacero. ISBN 9789568181093.

Di Sarno L, Elnashai AS, Nethercot DA. (2003). Seismic performance of stainless steel frames. Journal of Constructional Steel Research, 2003; 59(10): 1289-319.

Di Sarno L, Elnashai AS, Nethercot DA. (2005). Seismic response and design of stainless steel frames. Advances in Steel Structures, 2005, Vol. II: 1253-1258.

Di Sarno L, Elnashai AS, Nethercot DA. (2008). Seismic response of stainless steel braced frames. Journal of Constructional Steel Research, 2008, 64: 914-925.

Di Sarno L, Elnashai AS, Nethercot DA. (2006). Seismic retrofitting of Steel structures with stainless steel. Journal of Constructional Steel Research, 2006, 62(1): 93-104.

EN 10088. (2005). Stainless steels: list of stainless steels. Brussels: CEN, 2005.

EN-1998. (2004). Eurocode 8: Design of structures for earthquake resistance. Brussels: CEN, 2004.

IGC. (2011). Institut geològic de Catalunya. Terremoto de Lorca de 11 de mayo de 2011: Fuente sísmica y registros. Coloquio sobre implicaciones del sismo de Lorca (11 de mayo de 2011). Barcelona: 2011.

Munich RE. (2012). Earthquake, flood, nuclear accident. Topics GEO: Natural catastrophes 2011, analyses, assessments, positions. 2012.

NCSE-02. **(2002).** Norma de construcción sismorresistente: Parte general y edificación. Madrid: Ministerio de fomento, 2002.

Rasmussen AN. (2011). Steel Tower for a Wind Turbine, Patent US 20110271634 A1. [Online] Available at: <http://www.google.com/patents/US20110271634> [Accessed 5 February 2014].

Rossi B. (2014). Discussion on the use of stainless steel in constructions in view of sustainability. Elsevier, 2014.

Steel construction institute. (2006). Design Manual for Structural Stainless Steel. 3rd Edition. 2006. ISBN 2879972043.